MISCELLANEOUS PAPER C-77-I

ENGINEERING CONDITION SURVEY AND STRUCTURAL INVESTIGATION OF MARSH ARCH BRIDGE, FORT RILEY, KANSAS

by

T. C. Liu

Concrete Laboratory
U. S. Army Engineer Waterways Experiment Station
P. O. Box 631, Vicksburg, Miss. 39180

January 1977
Final Report

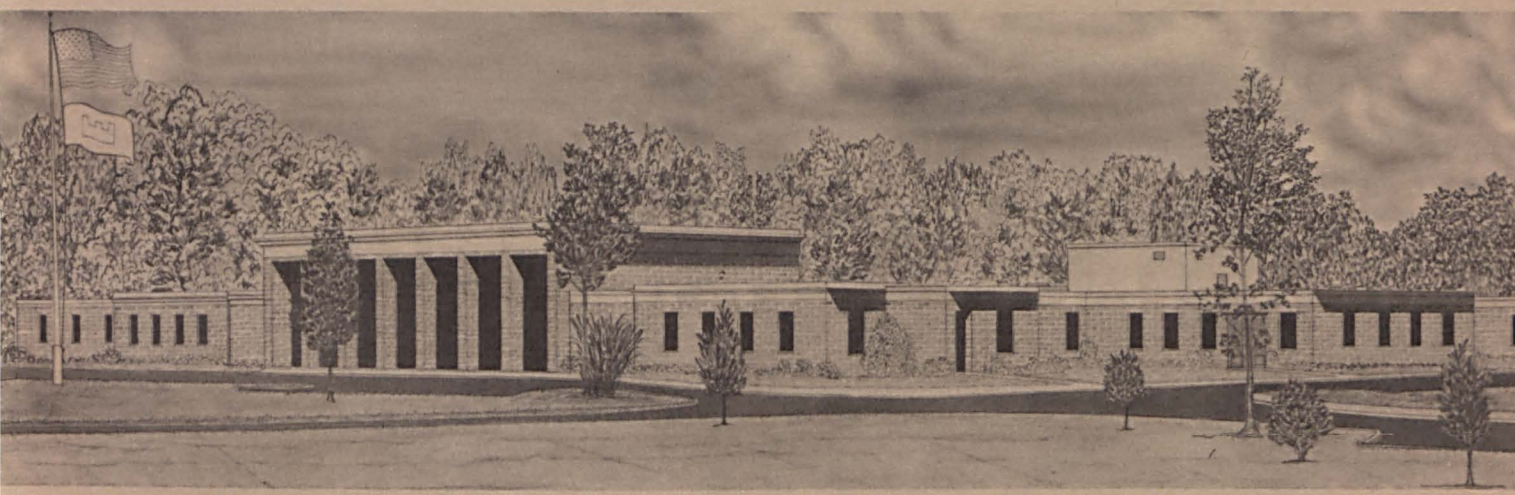

Prepared for U. S. Army Engineer District, Kansas City
Kansas City, Mo. 64106

Unclassified

SECURITY CLASSIFICATION OF THIS PAGE *(When Data Entered)*

REPORT DOCUMENTATION PAGE

READ INSTRUCTIONS BEFORE COMPLETING FORM

1. REPORT NUMBER: Miscellaneous Paper C-77-1	2. GOVT ACCESSION NO.
3. RECIPIENT'S CATALOG NUMBER	
4. TITLE *(and Subtitle)*: Engineering Condition Survey and Structural Investigation of Marsh Arch Bridge, Fort Riley, Kansas	5. TYPE OF REPORT & PERIOD COVERED: Final Report
6. PERFORMING ORG. REPORT NUMBER	
7. AUTHOR(s): T. C. Liu	8. CONTRACT OR GRANT NUMBER(s)
9. PERFORMING ORGANIZATION NAME AND ADDRESS: US Army Engineer Waterways Experiment Station, Concrete Laboratory, P. O. Box 631, Vicksburg, MS 39180	10. PROGRAM ELEMENT, PROJECT, TASK AREA & WORK UNIT NUMBERS
11. CONTROLLING OFFICE NAME AND ADDRESS: US Army Engineer District, Kansas City, Kansas City, MO 64106	12. REPORT DATE: January 1977
	13. NUMBER OF PAGES: 64
14. MONITORING AGENCY NAME & ADDRESS *(if different from Controlling Office)*	15. SECURITY CLASS. *(of this report)*: Unclassified
	15a. DECLASSIFICATION/DOWNGRADING SCHEDULE

16. DISTRIBUTION STATEMENT *(of this Report)*

Approved for public release, distribution unlimited.

17. DISTRIBUTION STATEMENT *(of the abstract entered in Block 20, if different from Report)*

18. SUPPLEMENTARY NOTES

19. KEY WORDS *(Continue on reverse side if necessary and identify by block number)*

Arch bridges	Concrete deterioration
Bridges (Structures)	Concrete failure
Concrete bridges	Marsh Arch Bridge
Concrete cracking	Structural analysis

20. ABSTRACT *(Continue on reverse side if necessary and identify by block number)*

This report presents the results of an engineering condition survey and structural investigation of Marsh Arch Bridge over the Republican River at the west side of Fort Riley, Kansas.

A visual inspection of the bridge with special attention given to concrete cracking, spalling, and deterioration was performed. Fourteen concrete core samples were taken and laboratory tests were performed to determine the cause

DD FORM 1 JAN 73 1473 EDITION OF 1 NOV 65 IS OBSOLETE

Unclassified

SECURITY CLASSIFICATION OF THIS PAGE *(When Data Entered)*

20. ABSTRACT (Continued).

and extent of deterioration and to obtain mechanical properties necessary for stress analyses. Detailed stress analyses were performed to determine the stress conditions in the bridge.

Based on the results of this investigation, it can be concluded that the bridge is in an advanced state of deterioration and any practical repairs will not be economically feasible.

Although the bridge is still considered to be structurally adequate for the present traffic conditions (i.e., one-lane traffic with 10-ton load limit), catastrophic failure could occur in the not too distant future because the rate of the deterioration will be accelerated due to the existence of large concrete cracks and the exposure of the steel elements.

It is, therefore, recommended that an early action toward replacement of this bridge (both super- and substructures) be initiated.

THE CONTENTS OF THIS REPORT ARE NOT TO BE USED FOR ADVERTISING, PUBLICATION, OR PROMOTIONAL PURPOSES. CITATION OF TRADE NAMES DOES NOT CONSTITUTE AN OFFICIAL ENDORSEMENT OR APPROVAL OF THE USE OF SUCH COMMERCIAL PRODUCTS.

PREFACE

The engineering condition survey and structural investigation of Marsh Arch Bridge, Fort Riley, Kansas, was conducted for the US Army Engineer District, Kansas City, Corps of Engineers, by the Concrete Laboratory of the US Army Engineer Waterways Experiment Station (WES). Authorization for this investigation was given in DA Form 2544 dated 11 June 1976.

This investigation was performed under the direction of Messrs. B. Mather J. M. Scanlon, and J. E. McDonald, CL. The visual inspection of the bridge was performed by Drs. C. E. Pace and T. C. Liu. The structural analysis was performed by Mr. R. L. Campbell. The concrete core logs were prepared by Mr. S. Wong. The petrographic and chemical analyses were performed by Messrs. A. D. Buck and T. Husbands, respectively. Mechanical properties tests were performed by Mr. W. O. Tynes. Concrete core drilling operations were performed by Mr. D. Stone of the Kansas City District. This report was written by Dr. T. C. Liu.

The cooperation and assistance of Mr. R. Henry of the Kansas City District and LTC R. E. Petty, Director of Facilities Engineering, Fort Riley, Kansas, are greatly appreciated. Appreciation is also expressed to Mr. E. Wilkinson of the Kansas Department of Transportation for providing the design information and bridge survey data.

The Commander and Director of WES during the conduct of this investigati and the preparation and publication of this report was COL J. L. Cannon, CE. Mr. F. R. Brown was Technical Director.

CONTENTS

CONVERSION FACTORS, US CUSTOMARY TO METRIC (SI)
UNITS OF MEASUREMENT

US customary units of measurement used in this report can be converted to metric (SI) units as follows:

Multiply	By	To Obtain
inches	2.540000 E-02	metre
feet	3.048000 E-01	metre
pounds (mass)	4.535924 E-01	kilogram
pounds (force)	4.448222 E+00	newton
pounds (force) per square inch	6.894757 E-03	megapascals
kip	4.448222 E+03	newton
kip-ft	1.355818 E+03	newton-metre

ENGINEERING CONDITION SURVEY AND STRUCTURAL INVESTIGATION OF MARSH ARCH BRIDGE, FORT RILEY, KANSAS

PART I: INTRODUCTION

1. This report presents the results of an engineering condition survey and structural investigation of Marsh Arch Bridge over the Republican River at the west side of Fort Riley, Kansas. The investigation was conducted during the period from July 1976 through December 1976 by the US Army Engineer Waterways Experiment Station for the US Army Engineer District, Kansas City.

Purpose and Approach

2. The purpose of this investigation is to determine the repairability or nonrepairability of the Marsh Arch Bridge over the Republican River at Fort Riley, Kansas.

3. The overall approach for the investigation is as follows:

   a. Study available historical information on the bridge, e.g., design drawings, records of previous inspections, and repairs performed on the bridge.

   b. Perform field condition survey, i.e., visual inspection of all bridge components with special attention given to concrete cracking, spalling, and deterioration.

   c. Obtain concrete core samples and perform laboratory tests to determine the cause and extent of deterioration and to obtain mechanical properties necessary for stress analysis.

   d. Perform stress analysis to determine the stress conditions in the structure under the traffic loads.

   e. Evaluate repair methods if the structure is found to be sound enough to repair.

Historical Information

4. The Marsh Arch Bridge consists of two 140-ft* span concrete arches supported on a single pier and two abutments (Figure 1).

5. This bridge is a composite design. The concrete arch ribs are reinforced with four 5- by 3-1/2- by 5/16-in. steel angles, and the diagonal reinforcement is provided by 2-1/2- by 2- by 1/4-in. steel angles. The cross-section of the arch ribs varies from 30 in. by 32 in. at the arch crown to 30 in. by 84 in. at the abutment. The vertical hangers are 30 in. by 8-1/2 in. in dimension and are reinforced with four 2-1/2- by 2-1/2- by 1/4-in. steel angles. The width of the floor beams is 12 in. and the height of the floor beams varies from 21 in. to 24 in. The floor beam is reinforced with two 3- by 3- by 5/16-in. steel angles. The bridge deck is 8-1/2 in. thick. The longitudinal and transverse directions are reinforced with 5/8- and 1/2-in. square bars, respectively. The abutments and pier are supported on timber piles. The design details are given in Figure 2.

6. This bridge was constructed in 1918, and the entire structure received a shotcrete surface treatment in about 1958. Several asphalt overlays have been placed on the roadway surface. It is estimated approximately 8 in. of asphalt now covers the bridge deck.

7. This is a one-lane bridge (20-ft roadway width) carrying one direction traffic flow. Due to the deteriorated condition of the bridge, it has been limited to a maximum load of 10 tons since early 1976.

8. As a part of the bridge monitoring program, survey studies on relative settlements of the structure have been performed by the Kansas Department of Transportation for the last four years. The level shots were originally taken along the hubguard, however, following 1974, the deterioration was too extensive so the profile lines were shifted onto the roadway 3 ft from the face of the hubguard. A plot of the roadway elevation is given in Figure 3. These profiles do not indicate any drastic changes during the last four years.

---

*A table of factors for converting US customary units of measurement to metric (SI) units is given on page 4.

PART II: VISUAL INSPECTION

9. A visual inspection of the bridge was made on 23-25 August 1976. This visual inspection was made by walking across and underneath the bridge as much as possible without wading the river. Photographs were taken to record the conditions of the bridge. Special attention was paid to concrete cracking, spalling, and deterioration. The results of this inspection are summarized as follows:

a. Arch ribs. Large spalling of the shotcrete surface and the original concrete was noted on each arch rib near abutment (Figure 4). The exposed aggregate particles in the original concrete were loose in their sockets and pieces of mortar could be removed by hand. Some steel elements were exposed and severe corrosion on the exposed steel was apparent. Almost all arch ribs exhibited longitudinal splitting (Figure 5). Steel corrosion stains were apparent at the surface of the cracks.

b. Floor beams. Severe deteriorations (cracking and spalling) appeared on all floor beams. Concrete crack widths as large as 1/8 in. were noted. A feeler gage blade inserted into one of the cracks went approximately 2 in. which was probably less than half the depth of the crack. Spalling of original concrete at the junctions of vertical hanger and floor beam was prevalent (Figure 6a). Rebar and steel elements were exposed showing stratified corrosion (Figure 6b and 6c). At the surface of the crack, leaching of the calcium hydroxide and other material compounds was noted (Figure 7). It is believed that the vertical hanger and floor beam joints are the most critical areas. The failure of some of these joints appears imminent.

c. Vertical hangers. Vertical cracks appeared on almost all hangers (Figure 8). It can be seen from Figure 8 that the vertical cracks extended to the full height of the hangers. Corrosion stains at the surface of the cracks were apparent.

d. Deck. There are many deteriorated areas as viewed from the underside of the bridge deck. Large spalling of the shotcrete surface and the original concrete was noted on several locations (Figure 6b). Figure 9 shows the pattern or map crackings on the underside of the bridge deck. They vary in width from barely visible to well-defined openings. Most of the drain holes on the bridge deck were partially clogged and dark colored deposits appeared around the drain holes.

e. Abutments and pier. Cracking and spalling of shotcrete surface and original concrete were noted on the abutments and pier (Figures 10 and 11). Pattern crackings were also noted. Figure 11 shows the severe erosion at the base of the pier.

PART III: LABORATORY TESTS

10. Since the depth and extent of concrete deterioration, as well as materials properties necessary for stress analysis, cannot be determined by visual inspection, laboratory tests on concrete core samples were considered necessary.

11. Fourteen 6-in. diameter concrete cores were taken from the abutments, arch rib, and bridge deck. The locations and orientations of these core samples are given in Table 1. When the 6-in diameter core samples were received at the Concrete Laboratory, photographs were taken (Figures 12-14) to illustrate the as received conditions. Detailed logs for each core were then prepared to record the concrete conditions and to identify the locations of cracks (Appendix A). The representative core samples were selected for petrographic examination, chemical analysis, and mechanical properties tests.

Petrographic Examination

12. The purpose of the petrographic examination was to determine the reason(s) for the deterioration of the concrete. Five concrete cores (3, 5, 6, 9, and 11) were selected for detailed petrographic examination. A complete petrographic examination report including test procedures and results is given in Appendix A. The results are summarized as follows:

a. The carbonate coarse aggregate is impure limestone composed of calcite with a small amount of quartz.

b. The concrete shows many closely spaced cracks which tend to parallel the concrete surfaces. These cracks traverse both the mortar and many of the coarse aggregate particles. The depth of damage due to this cracking ranges from about 1/2 to 1 ft in depth from the exterior core surfaces. The entire thickness of the bridge deck as represented by the concrete cores from the deck shows damage.

c. The sawed and ground surfaces of portions of cores 3 and 6 clearly show the presence of reaction rims on some chert particles and on some limestone particles. These rims, plus the detection of dried alkali-silica gel on broken surfaces, are clear evidence that both alkali-silica and alkali-carbonate rock reactions have occurred.

d. The cracking and deterioration of the concrete are due primarily to frost damage. It should be noted that the frost damage is not unusual for the nonair-entrained concrete exposed to the severe climate where freezing and thawing are common occurrences. It is believed that the deterioration of the concrete due to frost damage will be accelerated due to the existence of concrete cracks.

Chemical Analysis

13. Two concrete cores obtained from bridge deck (cores 12 and 14) were analyzed for chloride content. The top section, approximately 2 in. of each core, which appeared to be a concrete overlay, was sawed off to obtain a sample of the overlay. The sections sawed off from core 12 and 14 were designated as samples 12-A and 14-A, respectively. The top 1-1/2 in. of the remaining cores were sawed off to obtain a sample of the concrete below the overlay and were designated as samples 12-B and 14-B. The samples were then ground and blended so that a representative sample could be obtained.

14. The chloride content of each sample was determined using the procedures outlined in Appendix B. The test results are summarized below.

Sample	Percent Chloride
12-A	0.02
12-B	0.03
14-A	0.01
14-B	0.01

The amount of chloride in the concrete is considered to be very low and should not contribute to the corrosion of the steel elements.

Mechanical Properties Tests

15. Seven concrete cores (1, 2, 3, 6, 7, 13, and 15) were selected for mechanical properties tests. Cores 1, 2, 6, and 7 were first sawed to approximately 12 in. long (ratio of length of core to diameter L/D = 2) and cores 3, 13, and 15 were sawed to approximately 6 in. long (L/D = 1). All sawed cores were then submerged in lime-saturated water at 73 F per

CRD-C 27-69,[1] Standard Method of Obtaining and Testing Drilled Cores and Sawed Beams of Concrete. After 48 hr of soaking, the cores were removed from the lime-saturated water and capped with sulfur mortar in accordance with the applicable sections of CRD-C 29-74,[1] Standard Method of Capping Cylindrical Concrete Specimens. Cores having L/D = 2 were then tested to determine the compressive strength and static modulus of elasticity in accordance with the applicable provisions of CRD-C 14-73,[1] Standard Method of Test for Compressive Strength of Cylindrical Concrete Specimens, and CRD-C 19-75,[1] Standard Method of Test for Static Modulus of Elasticity and Poisson's Ratio of Concrete in Compression, respectively. Concrete cores having L/D = 1 were tested to determine the compressive strength per the applicable provisions of CRD-C 14-73.[1]

16. The results of these tests are presented in Table 2. It can be seen that compressive strength results ranged from 3850 to 2320 psi with an average of 2980 psi. Values of the modulus of elasticity ranged from 1.45×10^6 to 1.25×10^6 psi with an average of 1.34×10^6 psi. It is noted from Table 2 that the core samples tested had an unusually low modulus of elasticity which may be attributed to the existence of internal cracks.

17. The average values of compressive strength and modulus of elasticity (2980 psi and 1.34×10^6 psi, respectively) are used in the stress analysis and evaluation (Part IV).

PART IV: STRESS ANALYSIS AND EVALUATION

Stress Analysis

18. The purpose of the stress analysis is to determine the stress conditions in the structure and to evaluate whether the structural elements are over-stressed under the traffic loads.

19. The stress analysis was performed using the STRESS[2] computer program. The STRESS program is capable of analyzing structures in two or three dimensions, with either pinned or rigid joints, with prismatic or nonprismatic members, and subjected to concentrated or distributed loads, support motions, or temperature effects.

20. In the analysis, the Marsh Arch Bridge was considered as two-dimensional plane frame structure. The mathematical model of the bridge is shown in Figure 15. The model consists of 32 joints and 45 members. All supports are considered fixed. The member properties used in the analysis are given in Table 3. The dead, live, and impact loads are considered in the analysis. The dead load consists of the weights of the arch ribs, floor beams, bridge deck (including 8 in. of asphalt overlays), vertical hangers, and rail members. The live loads include the standard AASHO truck loads and lane loads for both HS20 and H10 loadings.[3] The impact effect of the live load is calculated according to the following formula.[3]

$$I = \frac{50}{L+125} \qquad (1)$$

where I = impact fraction (maximum 30 percent)

L = length in feet of the portion of the span which is loaded to produce the maximum stress in the member

Forty-six loading combinations were analyzed to determine the maximum stresses in the bridge elements (Table 4).

21. Based on the results of the stress analyses, the maximum member forces for both AASHO H10 and HS20 loadings are summarized in Table 5.

Structural Evaluation

Arch Ribs

22. Assuming uncracked section, the maximum extreme fiber stresses in arch rib elements can be calculated by the following equation:

$$\sigma_c = \frac{P}{A} \pm \frac{Mc}{I} \tag{2}$$

where σ_c = Extreme fiber stresses

P = Axial load (from Table 5)

A = Cross-sectional area of the member (from Table 3)

M = Bending moment (from Table 5)

c = Distance from neutral axis to the extreme fiber

I = Moment of inertia of the section (from Table 3)

23. Using Equation (2), the maximum extreme fiber stresses in arch rib elements for both AASHO H10 and HS20 loadings are calculated and presented in Table 6. It can be seen from Table 6 that all arch rib elements are in compression and within the allowable limit specified in AASHO Specifications.[3] Since all arch rib elements are in compression, the assumption of uncracked section is correct and the above analysis applies.

Vertical Hangers

24. It can be seen from Table 5 that all hanger members (member Nos. 5, 8, 11, 14, 17, 20, and 23) are subjected to tension plus bending. It is reasonable to assume that concrete offers no tensile resistance and all member forces are resisted by the steel elements only. The maximum steel stress in the hanger can be calculated as follows:

$$\sigma_s = \frac{P}{A_s} + \frac{M}{A_s e} \tag{3}$$

where σ_s = Steel stress

A_s = Total cross-sectional area of the steel elements

e = Distance from neutral axis to the centroid of tensile steel

and, all other terms are as defined in the previous paragraph.

25. The maximum steel stresses in the hanger members are calculated using Equation (3) and presented in Table 7. It can be seen from Table 7 that members 5 and 8 are overstressed under H10 loading and members 5, 8, 11, 20, and 23 are overstressed under HS20 loading. It should be noted, however, that the steel stresses presented in Table 7 are somewhat higher than the actual stresses because only the steel elements are considered in resisting the axial loads and bending moments.

Bridge Deck

26. It can be seen from Table 5 that the bridge deck elements are subjected to both axial tension and bending moments.* A cracked section was assumed in the analysis. It was further assumed that all axial tensile loads are resisted only by the steel elements. The steel stress and concrete stress can therefore be calculated as follows:[4]

$$\sigma_s = \frac{M}{A_s\ jd} + \frac{P}{A_s} \tag{4}$$

$$\sigma_c = \frac{M}{\frac{1}{2}bd^2\ kj} \tag{5}$$

where b = Half of the deck width

d = Effective depth of the deck

k = Ratio of distance between extreme fiber and neutral axis to effective depth

$$= \sqrt{2pn + (pn)^2} - pn$$

p = Ratio of area of tensile reinforcement to effective area of concrete

n = Ratio of modulus of elasticity of steel to that of concrete

j = Ratio of distance between resultants of compressive and tensile stresses to effective depth

$= 1 - k/3$, and

all other terms are as defined in the previous paragraphs.

---

*Except element 2 which is subjected to axial compression and bending.

27. Using Equations (4) and (5), the maximum steel and concrete stresses are calculated and given in Table 8. It can be seen that all stresses are within the allowable limits specified in Reference 3.

Floor Beams

28. Since a two-dimensional plane frame structure was assumed in the computer analysis, the forces in the floor beams cannot be determined. A hand calculation was therefore performed to determine the stress conditions in the floor beam. A 20-ft span rectangular beam fixed at both ends was assumed. The dead, live, and impact loads are considered in the calculation. It can be shown that the maximum end moments are 112 kip-ft and 80 kip-ft for AASHO HS20 and H10 loadings, respectively. Based on the design details given in Figure 2, the maximum rebar stresses in the floor beam are estimated[5] to be 18 ksi and 13 ksi for HS20 and H10 loadings, respectively. The maximum concrete stresses in the floor beams are 302 psi and 214 psi for HS20 and H10 loadings, respectively. These stresses are within the allowable limits specified in AASHO specifications.[3]

Deflections

29. Based on the results of the computer analysis, the maximum deflections at the center of the span are 0.85 in. and 0.96 in. for AASHO H10 and HS20 loadings, respectively. These deflections are considered acceptable.

PART V: SUMMARY, CONCLUSION, AND RECOMMENDATION

Summary

30. The results of this investigation are summarized as follows:

a. Visual inspection of both the super- and substructures revealed that cracking and spalling of the concrete structural elements were prevalent. It is believed that the vertical hanger and floor beam joints are the most critical areas. The failure of some of these joints appears imminent.

b. There are many closely spaced internal cracks due to frost damage. The depth of damage ranges from 1/2 to 1 ft from the exterior surfaces. It is also found that the entire thickness of the bridge deck is damaged.

c. The cracking and deterioration of the concrete are due primarily to frost damage, although both alkali-silica and alkali-carbonate rock reactions have occurred.

d. The amount of chloride in the concrete is considered to be very low and should not contribute to the corrosion of the steel elements.

e. The compressive strengths of the concrete core samples ranged from 3850 to 2320 psi with an average of 2980 psi. Values of the modulus of elasticity ranged from 1.45×10^6 to 1.25×10^6 psi with an average of 1.34×10^6 psi. The low modulus of elasticity may be attributed to the existence of internal cracks.

f. The results of the stress analyses indicated that, at the present condition, the bridge is capable of supporting AASHO H10 loadings. The AASHO HS20 loadings will grossly overstress the vertical hangers. It is, therefore, considered mandatory to limit the traffic to 10-ton load.

Conclusion and Recommendation

31. On the basis of this investigation, it can be concluded that the bridge is in an advanced state of deterioration, and any practical repairs will not be economically feasible.

32. Although the bridge is still considered to be structurally adequate for the present traffic conditions (i.e., one-lane traffic with 10-ton load limit), catastrophic failure could occur in the not too distant

future because the rate of the deterioration will be accelerated due to the existence of large concrete cracks and the exposure of the steel elements.

33. It is, therefore, recommended that an early action toward replacement of this bridge (both super- and substructures) be initiated.

REFERENCES

1. "Handbook for Concrete and Cement," US Army Engineer Waterways Experiment Station, Vicksburg, MS.
2. Fenves, S. J., et al., "STRESS: A User's Manual," MIT Press, Cambridge, MA.
3. "Standard Specification for Highway Bridges," AASHO, 10th Ed., 1969.
4. Winter, G., et al., "Design of Concrete Structures," 7th Ed., McGraw-Hill, New York, 1964.
5. "Reinforced Concrete Design Handbook," 3rd Ed., ACI Special Publication SP-3, 1965.

Table 1

Concrete Core Samples

No.	Location	Core Dimension (inches)	Core Orientation
1	Abutment (South End, Upstream)	6 x 18	Horizontal
2	Abutment (South End, Downstream)	6 x 18	Horizontal
3	Arch (South End, Downstream)	6 x 12	Horizontal
5	Abutment (North End, Upstream)	6 x 24	Horizontal
6	Abutment (North End, Center)	6 x 24	Horizontal
7	Abutment (North End, Downstream)	6 x 25	Horizontal
8	Bridge Deck (South End, Upstream)	6 x 8	Vertical
9	Bridge Deck (South End, Upstream)	6 x 8	Vertical
10	Bridge Deck (North End, Upstream)	6 x 12	Vertical
11	Bridge Deck (North End, Upstream)	6 x 12	Vertical
12	Bridge Deck (South End, Downstream)	6 x 8	Vertical
13	Bridge Deck (South End, Downstream)	6 x 8	Vertical
14	Bridge Deck (North End, Downstream)	6 x 8	Vertical
15	Bridge Deck (North End, Downstream)	6 x 8	Vertical

Table 2

Results of Mechanical Properties Tests

Core	Dimension (D x L) (inches)	Failure Load (lb)	Compressive Strength (psi)	Modulus of Elasticity (x 10^6 psi)
1	5.9 x 12.4	73,100	2,680	1.25
2	5.9 x 12.4	92,400	3,380	1.29
3	5.9 x 6.1	77,550	2,580*	----
6	5.9 x 12.4	75,300	2,760	1.38
7	5.9 x 11.3	105,000	3,850	1.45
13	5.9 x 6.1	99,600	3,320*	----
15	5.9 x 6.3	69,500	2,320*	----

* Correction factor of 0.91 was used in computing the compressive strengths per CRD-C 27-69[1]

Table 3

Member Properties

Member	Area (ft^2)	Moment of Inertia (ft^4)
1	11.50	20.28
2	7.32	0.306
3	7.32	0.306
4	9.00	9.72
5	1.77	0.074
6	7.32	0.306
7	8.00	6.83
8	1.77	0.074
9	7.32	0.306
10	7.50	5.63
11	1.77	0.074
12	7.32	0.306
13	7.25	5.08
14	1.77	0.074
15	7.32	0.306
16	7.00	4.57
17	1.77	0.074
18	7.32	0.306
19	6.83	4.24
20	1.77	0.074
21	7.32	0.306
22	6.75	4.1
23	1.77	0.074
24	7.32	0.306
25	6.75	4.1
26	1.77	0.074
27	7.32	0.306
28	6.83	4.24
29	1.77	0.074
30	7.32	0.306
31	7.00	4.57
32	1.77	0.074
33	7.32	0.306
34	7.25	5.08
35	1.77	0.074
36	7.32	0.306
37	7.50	5.63
38	1.77	0.074
39	7.32	0.306
40	8.00	6.83
41	1.77	0.074
42	7.32	0.306
43	9.00	9.72
44	11.50	20.28
45	7.32	0.306

Table 4

Loading Combinations

No.	Loading Combination	Class of Loading
1	DL + Lane Load + Concentrated Load at Joint 3 + Impact	H20 and HS 20
2	DL + Lane Load + Concentrated Load at Joint 4 + Impact	H20 and HS 20
3	DL + Lane Load + Concentrated Load at Joint 6 + Impact	H20 and HS 20
4	DL + Lane Load + Concentrated Load at Joint 8 + Impact	H20 and HS 20
5	DL + Lane Load + Concentrated Load at Joint 10 + Impact	H20 and HS 20
6	DL + Lane Load + Concentrated Load at Join 12 + Impact	H20 and HS 20
7	DL + Lane Load + Concentrated Load at Joint 14 + Impact	H20 and HS 20
8	DL + Lane Load + Concentrated Load at Joint 16 + Impact	H20 and HS 20
9	DL + Lane Load + Concentrated Load at Joint 3 + Impact	H10
10	DL + Lane Load + Concentrated Load at Joint 4 + Impact	H10
11	DL + Lane Load + Concentrated Load at Joint 6 + Impact	H10
12	DL + Lane Load + Concentrated Load at Joint 8 + Impact	H10
13	DL + Lane Load + Concentrated Load at Joint 10 + Impact	H10
14	DL + Lane Load + Concentrated Load at Joint 12 + Impact	H10

(Continued)

Table 4 (Continued)

No.	Loading Combination	Class of Loading
15	DL + Lane Load + Concentrated Load at Joint 14 + Impact	H10
16	DL + Lane Load + Concentrated Load at Joint 16 + Impact	H10
17	DL + Truck Load (Middle Axle at Joint 3) + Impact	HS 20
18	DL + Truck Load (Middle Axle at Joint 4) + Impact	HS 20
19	DL + Truck Load (Middle Axle at Joint 6) + Impact	HS 20
20	DL + Truck Load (Middle Axle at Joint 8) + Impact	HS 20
21	DL + Truck Load (Middle Axle at Joint 10) + Impact	HS 20
22	DL + Truck Load (Middle Axle at Joint 12) + Impact	HS 20
23	DL + Truck Load (Middle Axle at Joint 14) + Impact	HS 20
24	DL + Truck Load (Middle Axle at Joint 16) + Impact	HS 20
25	DL + Truck Load (Middle Axle at Joint 18) + Impact	HS 20
26	DL + Truck Load (Middle Axle at Joint 20) + Impact	HS 20
27	DL + Truck Load (Middle Axle at Joint 22) + Impact	HS 20
28	DL + Truck Load (Middle Axle at Joint 24) + Impact	HS 20
29	DL + Truck Load (Middle Axle at Joint 26) + Impact	HS 20

(Continued)

Table 4 (Continued)

No.	Loading Combination	Class of Loading
30	DL + Truck Load (Middle Axle at Joint 28) + Impact	HS 20
31	DL + Truck Load (Middle Axle at Joint 30) + Impact	HS 20
32	DL + Truck Load (Rear Axle at Joint 3) + Impact	H10
33	DL + Truck Load (Rear Axle at Joint 4) + Impact	H10
34	DL _ Truck Load (Rear Axle at Joint 6) + Impact	H10
35	DL + Truck Load (Rear Axle at Joint 8) + Impact	H10
36	DL + Truck Load (Rear Axle at Joint 10) + Impact	H10
37	DL + Truck Load (Rear Axle at Joint 12) + Impact	H10
38	DL + Truck Load (Rear Axle at Joint 14) + Impact	H10
39	DL + Truck Load (Rear Axle at Joint 16) + Impact	H10
40	DL + Truck Load (Rear Axle at Joint 18)	H10
41	DL + Truck Load (Rear Axle at Joint 20)	H10
42	DL + Truck Load (Rear Axle at Joint 22)	H10
43	DL + Truck Load (Rear Axle at Joint 24)	H10
44	DL + Truck Load (Rear Axle at Joint 26)	H10

(Continued)

Table 4 (Concluded)

No.	Loading Combination	Class of Loading
45	DL + Truck Load (Rear Axle at Joint 28)	H10
46	DL + Truck Load (Rear Axle at Joint 30)	H10

Table 5

Summary of Maximum Member Forces

Member	H10 Loading		HS20 Loading	
	Axial Load* (Kips)	Bending Moment (Kips-ft)	Axial Load* (Kips)	Bending Moment (Kips-ft)
1	-426.5	239.0	-459.7	291.5
2	-58.1	19.0	-67.5	20.4
3	+0.3	27.2	+0.1	30.7
4	-444.7	216.2	-469.9	266.3
5	+28.5	10.0	+36.0	13.3
6	+4.9	18.2	+5.6	20.9
7	-429.6	59.3	-457.9	70.7
8	+31.1	5.2	+37.8	7.3
9	+6.4	19.0	+7.4	21.4
10	-420.5	65.5	-448.3	73.7
11	+31.7	4.3	+38.4	4.8
12	+7.2	18.5	+8.2	21.0
13	-408.4	41.3	-435.6	54.2
14	+32.4	4.1	+39.0	3.5
15	+8.0	17.8	+9.1	20.4
16	-399.0	32.1	-425.8	43.9
17	+32.9	3.7	+39.5	3.6
18	+8.6	14.9	+9.9	16.9
19	-391.4	88.9	-417.7	119.3
20	+32.5	2.5	+39.0	4.1
21	+9.0	9.6	+10.4	10.9
22	-388.9	91.0	-415.2	120.7
23	+32.7	0.7	+39.3	4.2

* + Indicates tension
  - Indicates compression

Table 6

Maximum Concrete Stresses in Arch Ribs

Member	Maximum Extreme Fiber Stresses* H10 (psi)	Maximum Extreme Fiber Stresses* HS20 (psi)	Allowable Stress** (psi)
1	-69.5/-445.7	-48.0/-507.2	-1190
4	-65.1/-621.1	-20.2/-705.0	-1190
7	-276.4/-468.4	-282.5/-512.5	-1190
10	-268.1/-510.5	-278.7/-551.5	-1190
13	-309.3/-473.1	-309.8/-524.6	-1190
16	-327.5/-464.1	-329.0/-515.8	-1190
19	-199.2/-596.6	-158.0/-691.4	-1190
22	-192.0/-608.2	-151.1/-703.1	-1190

* Uncracked sections are assumed.

** Allowable stress = 0.4 f'_c 2

Table 7

Maximum Steel Stresses in the Hangers

Member	Maximum Steel Stresses* H10 Loading (Ksi)	Maximum Steel Stresses* HS20 Loading (Ksi)	Allowable Stress (Ksi)
5	35.7	47.0	20.0
8	22.0	29.6	20.0
11	19.4	22.3	20.0
14	19.0	18.6	20.0
17	17.9	19.0	20.0
20	14.2	20.4	20.0
23	9.0	20.7	20.0

*Use 4 Ls - 2-1/2 in. x 2-1/2 in. x 1/4 in. (Figure 2)
$A_s = 4 \times 1.19 = 4.76$, $e = 0.85$ in.

Table 8

Maximum Stresses in the Bridge Deck Elements

Member	Maximum Stresses*				Allowable Stresses	
	H10 Loading		HS20 Loading			
	Concrete Stress (psi)	Steel Stress (Ksi)	Concrete Stress (psi)	Steel Stress (Ksi)	Concrete (psi)	Steel (Ksi)
2	-223	-2.0	-240	-2.9	-1190	±20
3	-319	+7.7	-360	+8.7	-1190	±20
6	-214	+5.8	-245	+6.6	-1190	±20
9	-223	+6.2	-251	+7.0	-1190	±20
12	-217	+6.1	-246	+7.0	-1190	±20
15	-209	+6.0	-239	+6.9	-1190	±20
18	-175	+5.3	-198	+6.0	-1190	±20
21	-113	+3.9	-128	+4.4	-1190	±20

*- indicates compression; + indicates tension

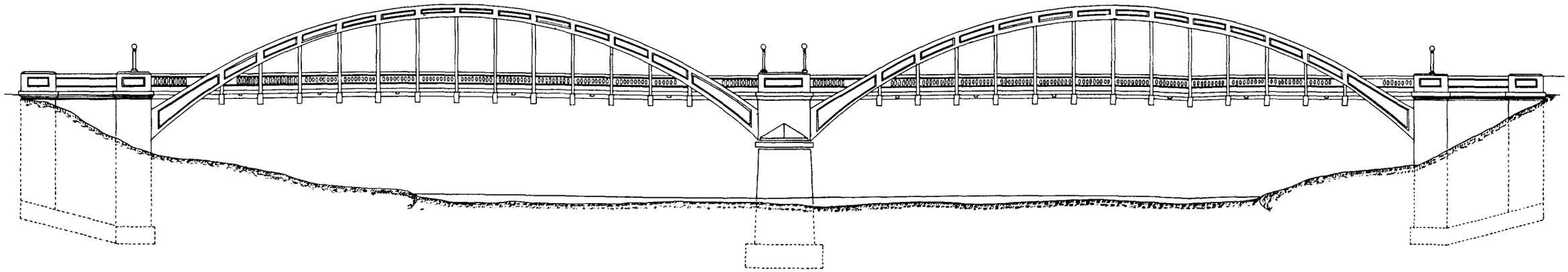

SIDE ELEVATION

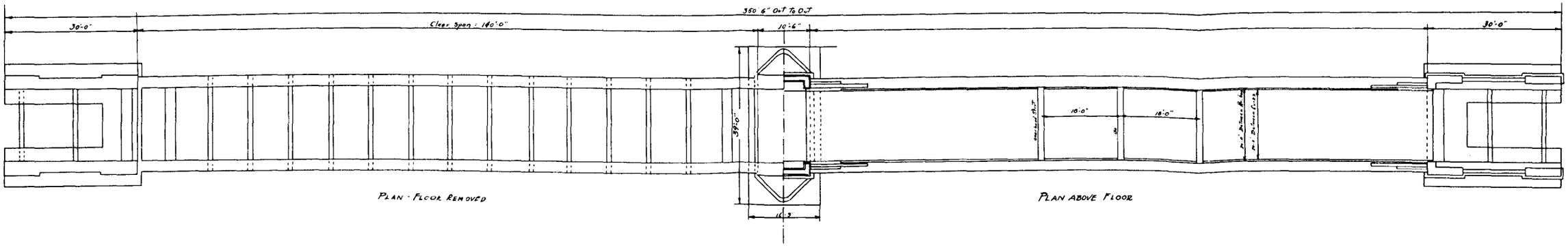

PLAN - FLOOR REMOVED

PLAN ABOVE FLOOR

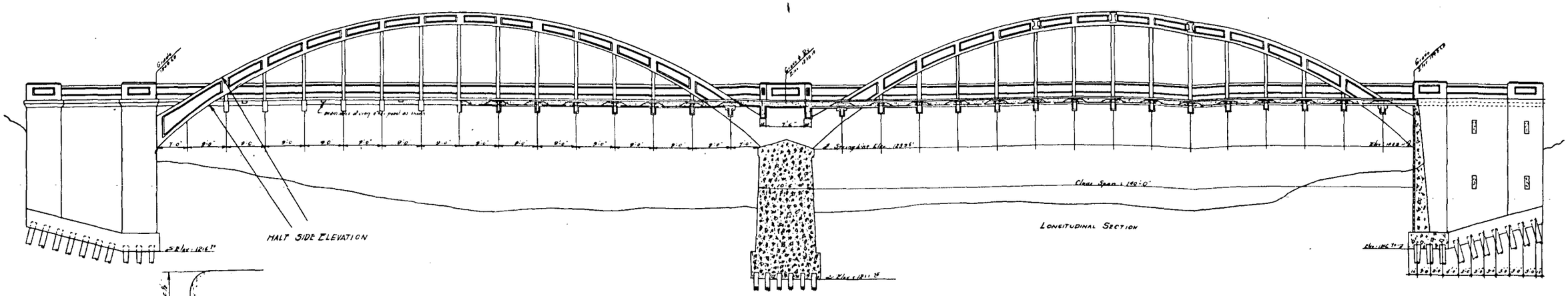

HALF SIDE ELEVATION

LONGITUDINAL SECTION

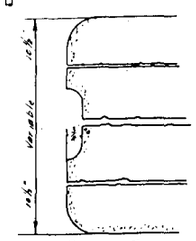

PART SEC OF ARCH

Design for
MARSH RAINBOW ARCH BRIDGE
over
REPUBLICAN RIVER
Ft Riley KANSAS
Scale 1/8 : 1'-0" November 1917
MARSH ENGINEERING Co
DES MOINES IOWA
Sheet-4/4
U File A4 12

Submitted by
Leavenworth Bridge Co
Leavenworth Kan 583

Retraced by Q.M.C. Ft Riley Kan
June 8 1918

Figure 1. Marsh Arch Bridge

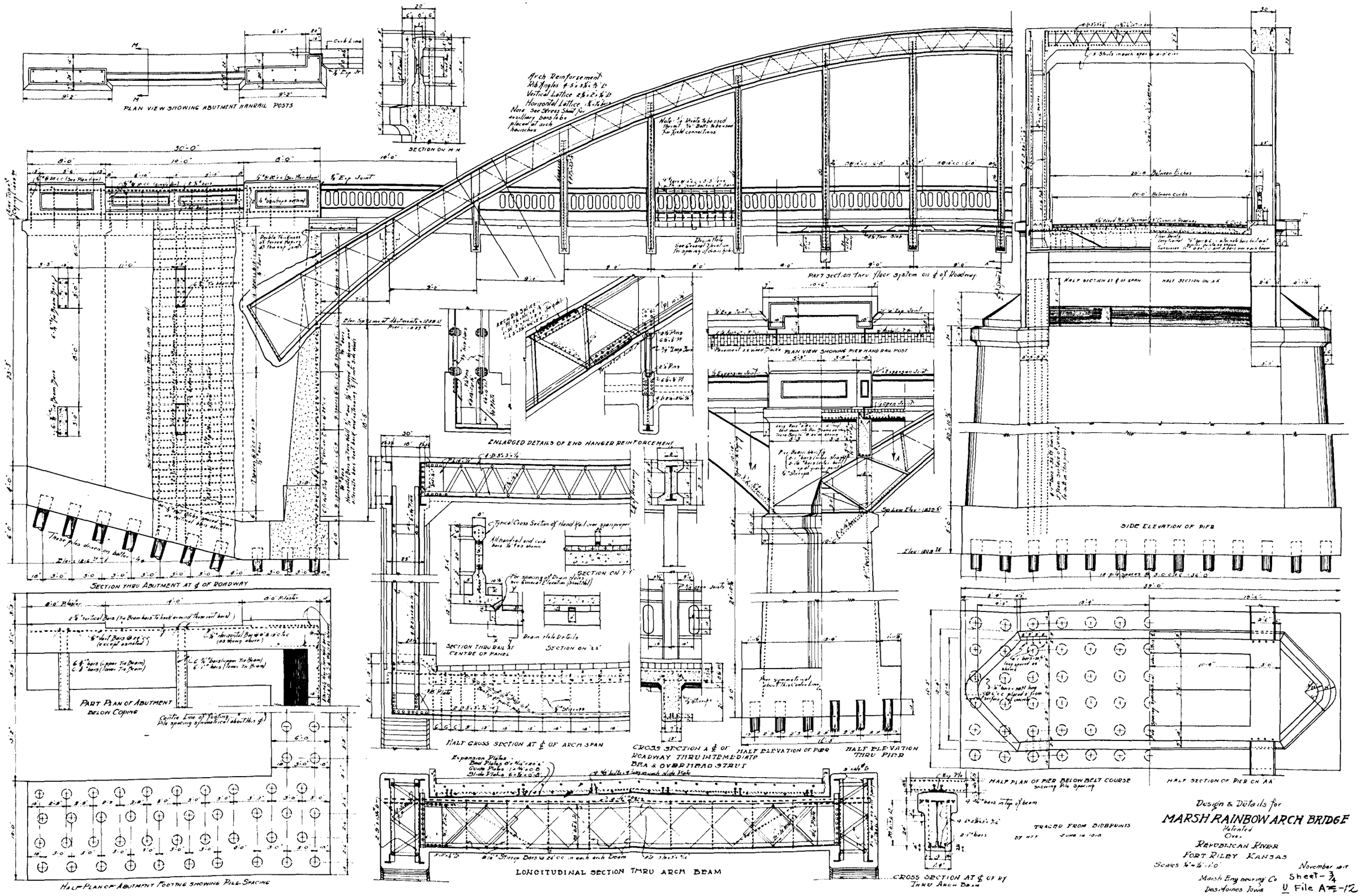

Figure 2. Design details for Marsh Arch Bridge

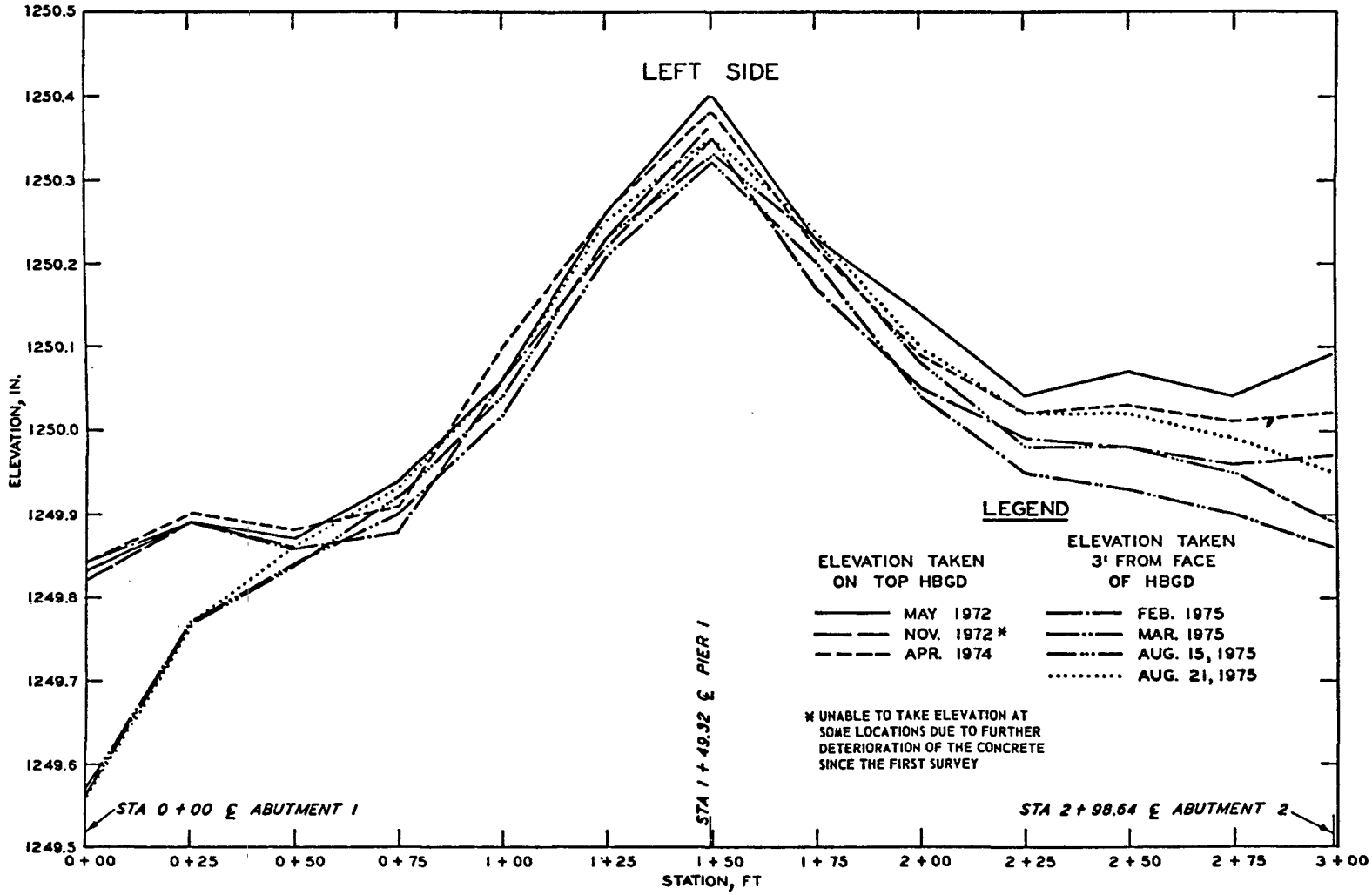

Figure 3a. Bridge roadway elevations (Courtesy of the Kansas Department of Transportation).

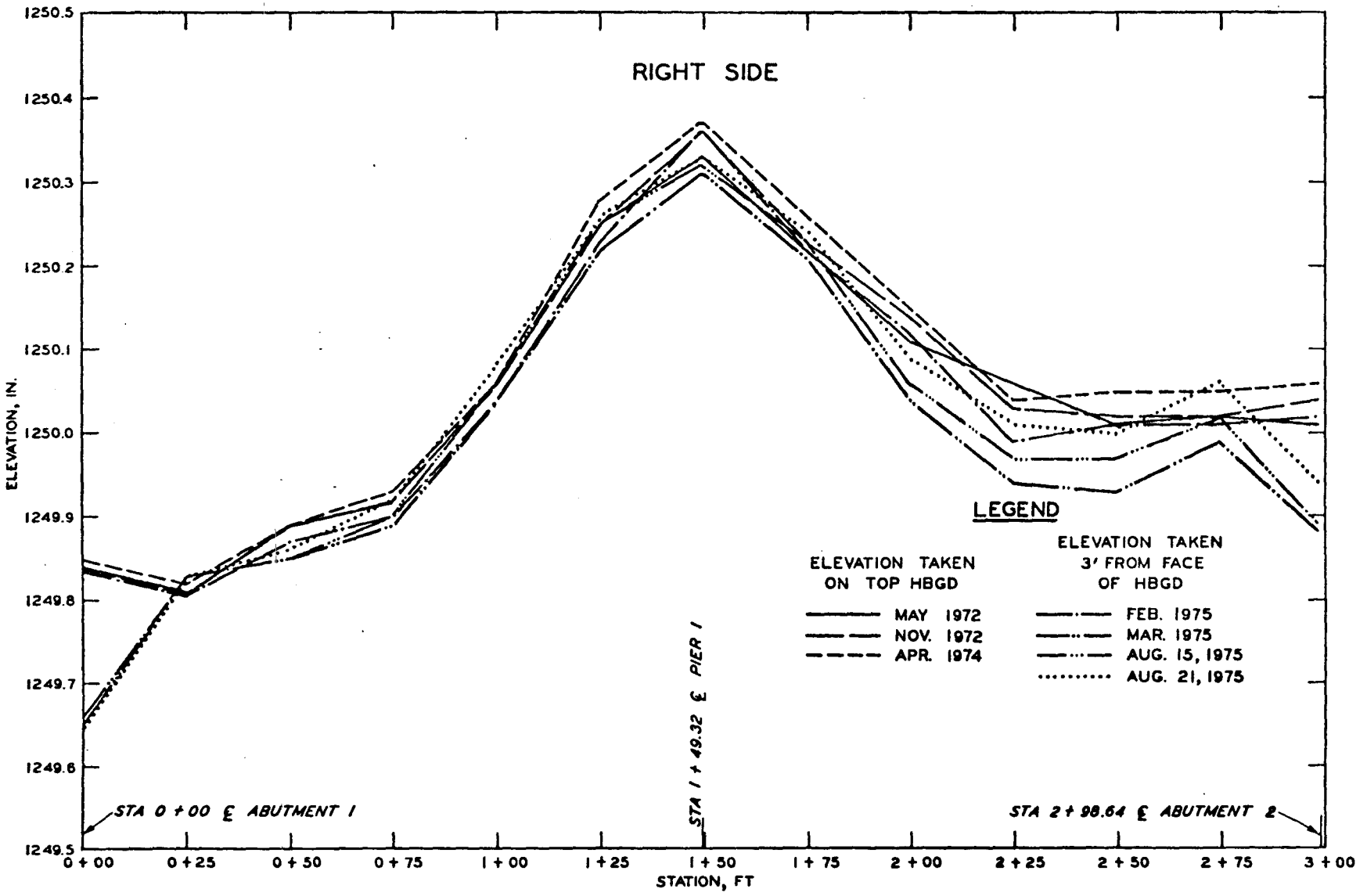

Figure 3b. Bridge roadway elevation (Courtesy of the Kansas Department of Transportation).

a. South end, downstream

b. North end, upstream

Figure 4. Arch rib near abutment showing large spalling. (Note exposure of steel)

a. Cracks running parallel with arch

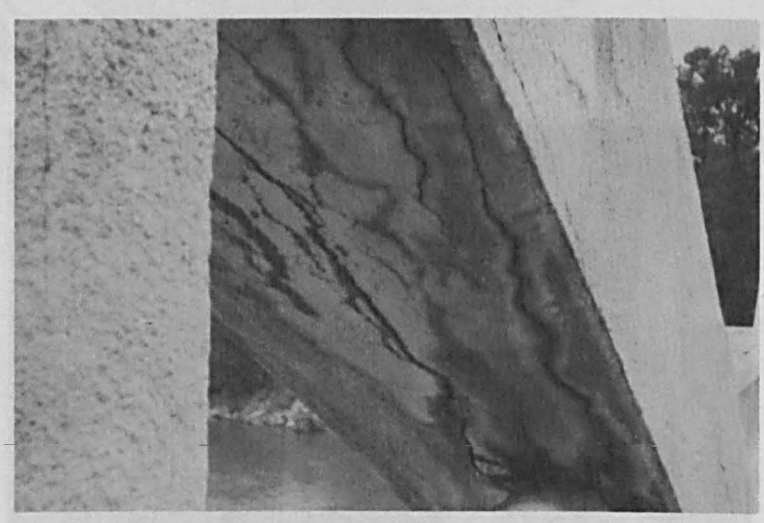

b. Heavy rust stain at surface of cracks

Figure 5. Cracking of arch rib

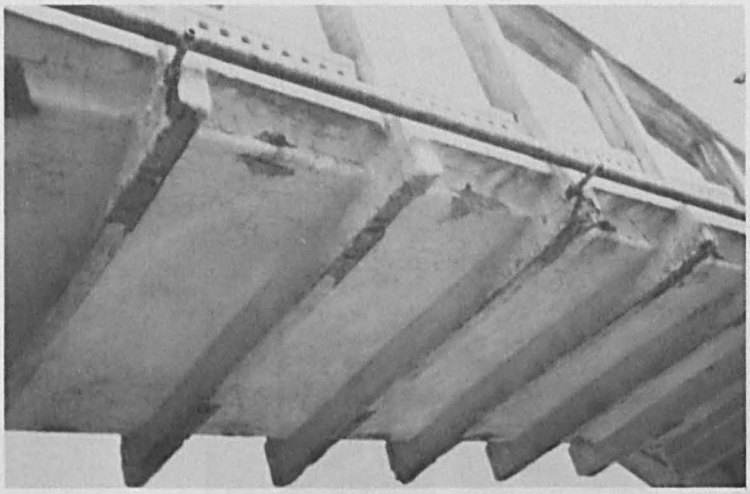

a. Overall view. (The utility line is anchored to the floor beams)

b. Exposure of rebar and steel elements

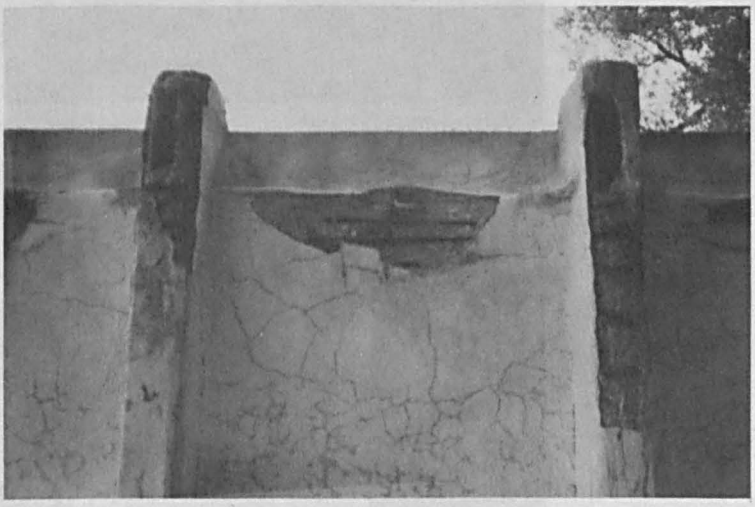

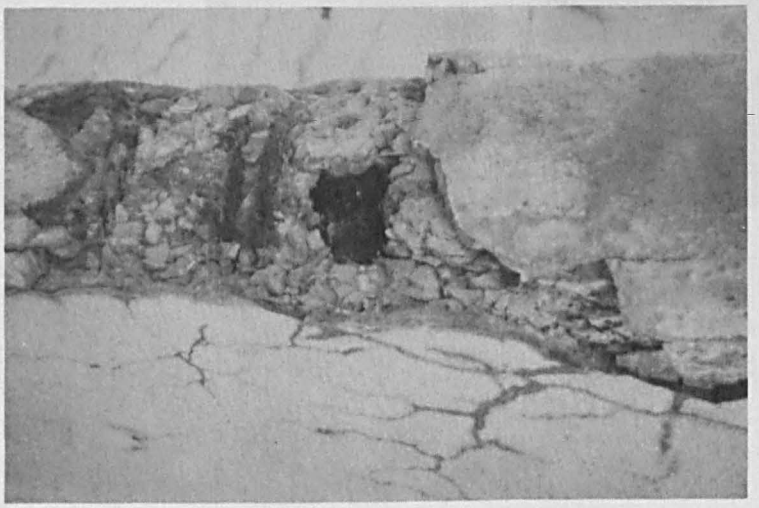

c. Closeup of a typical deteriorated floor beam

Figure 6. Floor beams showing spalling and cracking

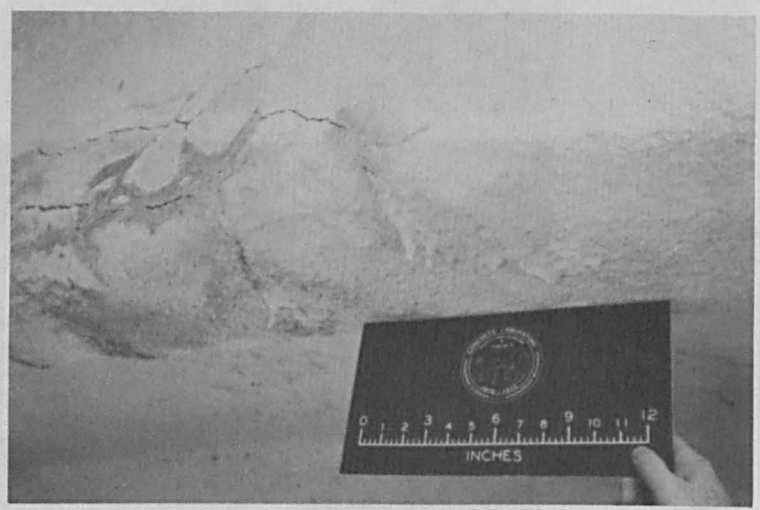

Figure 7. Leaching of floor beam

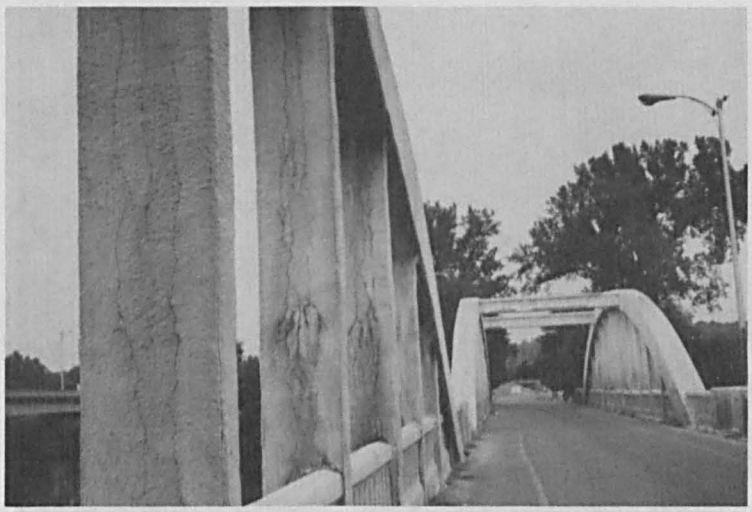

a. Overall view

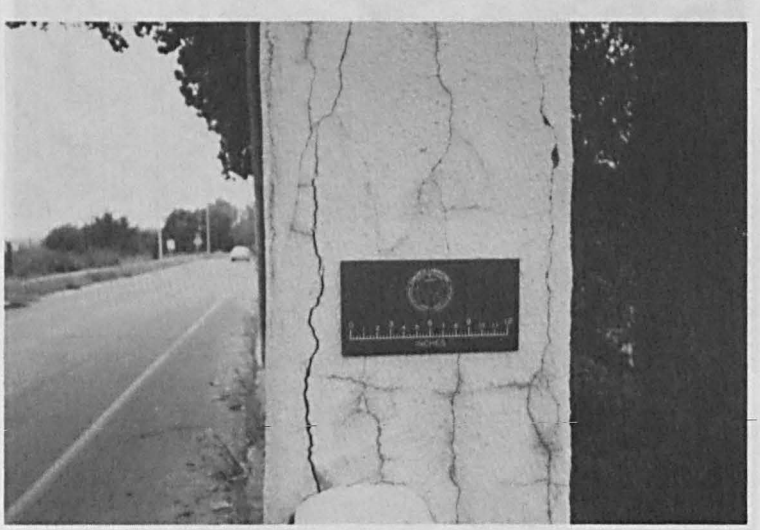

b. Closeup view

Figure 8. Cracks in vertical hangers

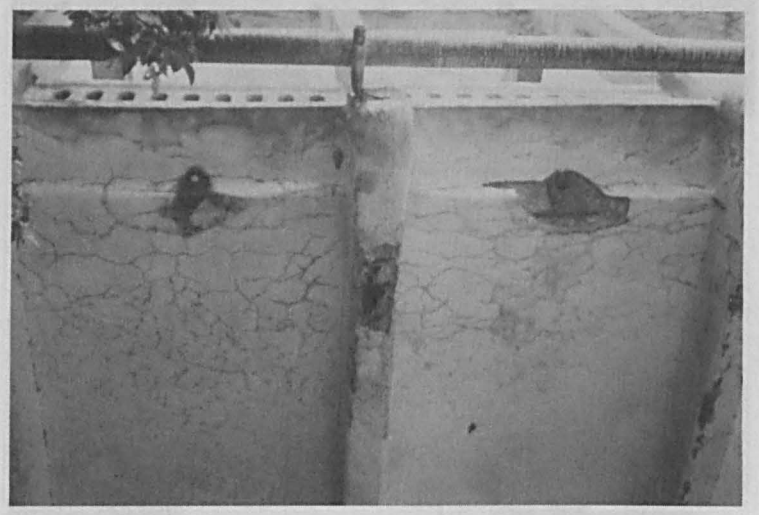

Figure 9. Underside of bridge deck

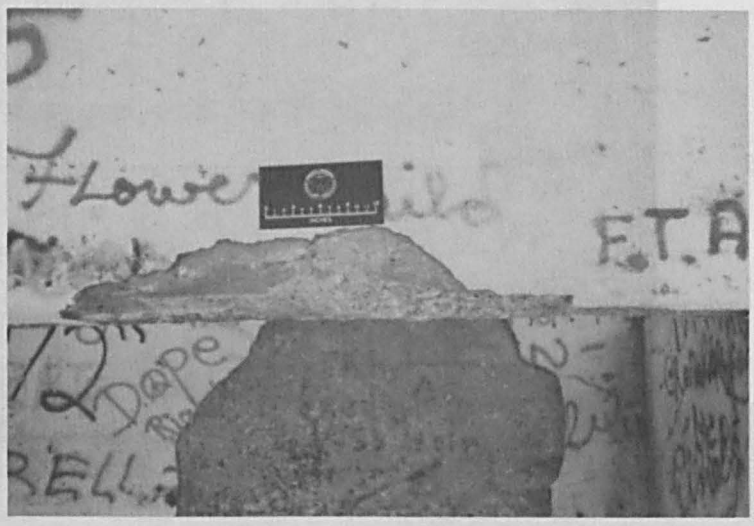

Figure 10. Large spalling of shotcrete surface of abutment

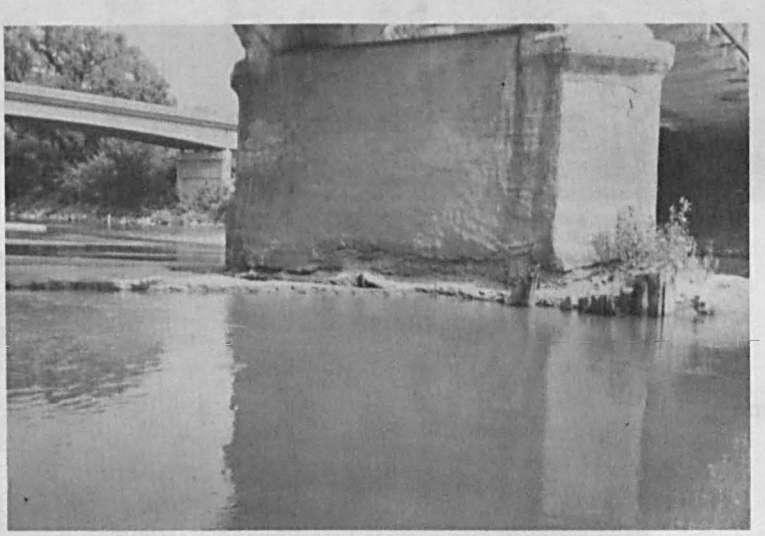

Figure 11. Severe erosion at base of pier

a. South end
(cores 1 and 2)

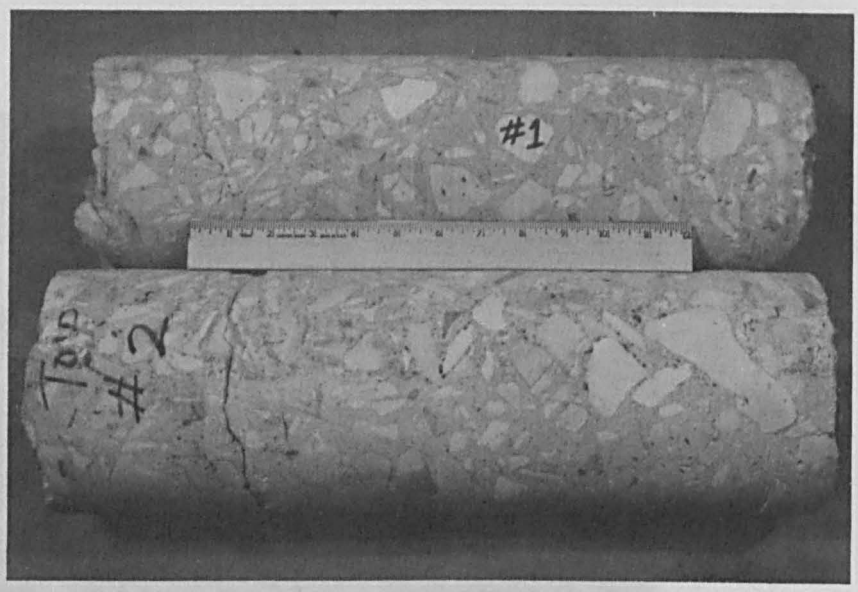

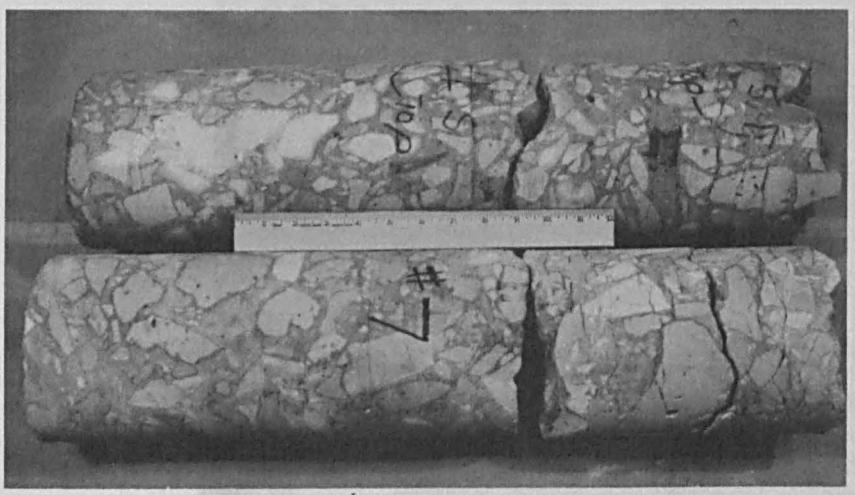

b. North end
(cores 5 and 7)

c. North end
(core 6)

Figure 12. Concrete cores drilled from abutment

Figure 13. Concrete core drilled from arch rib (south end, downstream)

a. South span (cores 8, 9, 12, and 13)

b. North span (cores 10, 11, 14, and 15)

c. Closeup showing cracks

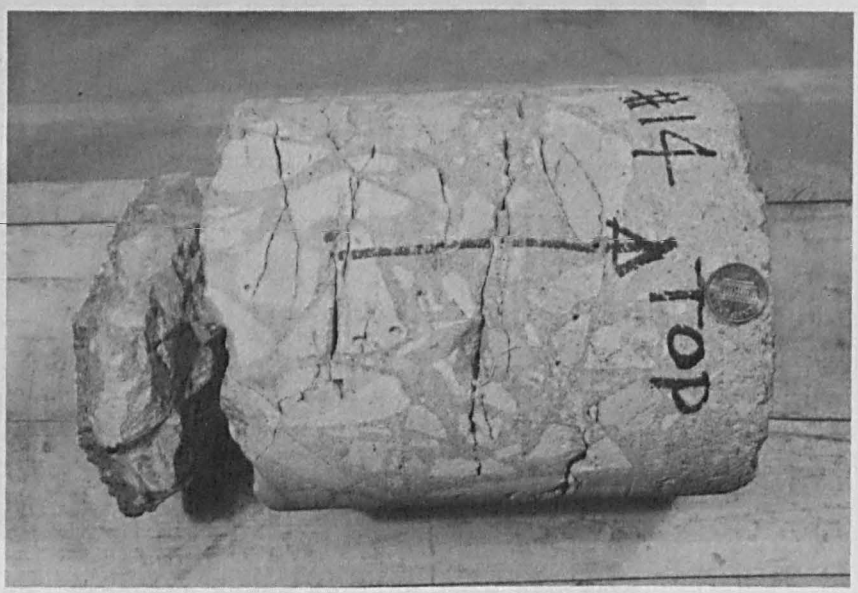

Figure 14. Concrete cores drilled from bridge deck

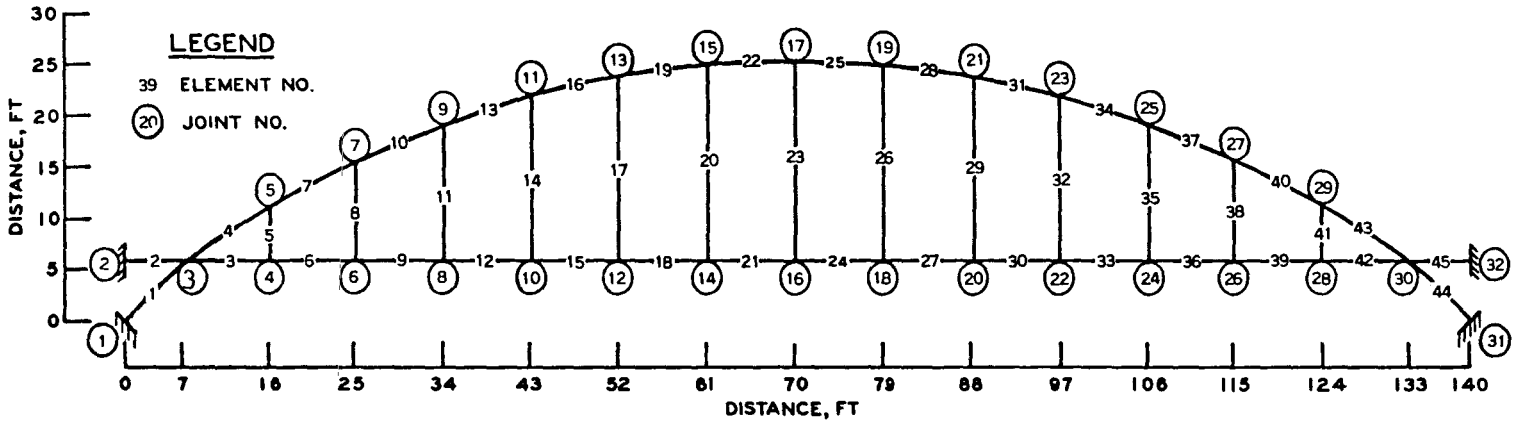

Figure 15. Mathematical model of the Marsh Arch Bridge.

APPENDIX A

PETROGRAPHIC REPORT

Corps of Engineers, USAE Waterways Experiment Station	Petrographic Report	Concrete Laboratory P. O. Box 631 Vicksburg, Mississippi
Project Examination of Concrete Cores, Marsh Arch Bridge, Fort Riley, Kansas		Date 19 November 1976 ADB

Samples

1. Fragments of concrete and 14 concrete cores of 6-in. diameter were received in August and October 1976 for petrographic examination and other tests. The petrographic examination was made to determine the reason or reasons for the deterioration of the concrete.

2. The cores are identified below:

Field No.	Description
1, 2	South Abutment
3	Arch
5, 6, 7	North Abutment
8 thru 15	Bridge Deck

The first seven cores were taken horizontally, and the remainder were vertical cores. No. 4 is missing from the above sequence because the drilling of it was cancelled.

Test procedure

3. The fragments of concrete which included some shotcreted pieces were examined with a stereomicroscope.

a. Portions from two pieces of chert from the coarse aggregate were used in powder immersion mounts which were examined with a polarizing microscope to determine if they were chalcedonic and thus potentially reactive material.

b. Three of the carbonate coarse aggregate particles were examined separately by X-ray diffraction to determine their composition. Each piece was ground to pass a 45 μm sieve before being X-rayed.

c. A portion of the cement paste was concentrated by crushing scraps of the old mortar and passing it over a 150 μm sieve. The finer material was then ground to pass a 45 μm sieve and was X-rayed. Since this material was so carbonated the procedure was repeated using freshly broken surfaces of core 3.

4. The cores were inspected and logged. All or portions of cores 3 (Arch), 5 and 6 (North Abutment), and 9 and 11 (Bridge Deck) were selected for additional examination. These samples were examined with a stereomicroscope. A longitudinal slice was cut from cores 3 and 5. One surface of each slice was ground to provide a high quality surface which was inspected by stereomicroscope. Photographs were taken of these surfaces to show reacted coarse aggregate particles. A small amount of alkali-silica gel was removed from a broken surface of core 3 and examined as a powder immersion mount.

5. A portion of the white mortar coating the shotcreted surfaces was ground and X-rayed. All X-ray examinations were made with an X-ray diffractometer using nickel-filtered copper radiation.

Results

6. Earlier inspection of the fragmented material showed:

a. The refractive index of the chert that was checked was lower than 1.544. Thus, it is potentially reactive in the alkali-silica reaction.

b. The carbonate coarse aggregate is impure limestone composed of calcite with a small amount of quartz.

c. The cement paste is largely carbonated. The X-ray pattern showed a little calcium carboaluminate and abundant calcite. There was no detectable calcium hydroxide or ettringite. The X-ray examination of a paste concentrate from fresh fracture surfaces of core 3 showed this paste was not carbonated. It contained ettringite, calcium hydroxide, and probably two forms of calcium carboaluminate. While the latter material was a little more abundant than usual, the overall composition of the paste was essentially normal.

d. The shotcrete was well bonded to the old concrete in the samples that were examined. The X-ray examination of the white mortar coating suggested that it contained a white cement.

e. There were several small samples of white encrustations. These were stalactite-like forms composed of calcite. They probably formed by leaching of lime from the concrete with subsequent deposition on concrete surfaces and later conversion to calcite.

7. The logs of the cores are shown in Figures A1 through A14. The concrete shows many fairly closely spaced cracks which tend to parallel the formed concrete surfaces. These cracks traverse both the mortar and many of the coarse aggregate particles of the concrete. The depth of damage due to this cracking ranges from about 1/2 to 1 ft in depth from the exterior core surfaces. In general, one could say that the entire thickness of the bridge deck as represented by the eight cores from the deck shows damage. The presence of cracks such as these in old nonair-entrained concrete is sufficient evidence of frost damage.

8. The sawed and ground surfaces of portions of cores 3 and 6 are shown in Figure A15. These surfaces clearly show the presence of reaction rims on some chert particles and on some limestone particles. These rims, plus the detection of dried alkali-silica gel on broken surfaces, are clear evidence that both alkali-silica and alkali-carbonate rock reactions have occurred. A powder immersion mount of the gel showed it to consist of transparent and brownish types with refractive indices below 1.544. The transparent type shows a salt and pepper type texture under crossed nicols and is probably crystalline.

9. The alkali-carbonate rock reaction associated with nondolomitic limestone similar to this coarse aggregate is not usually thought to produce deleterious expansion and cracking.* Therefore, the cracking and deterioration of this concrete is due to frost damage and/or to alkali-silica reaction. The type of cracking suggests that the major portion of the damage or all of the damage is due to frost action which was harmful to the nonair-entrained concrete.

---

* Department of the Army, Office, Chief of Engineers, "Standard Practice for Concrete," Engineer Manual EM 1110-2-2000, Appendix C, 1 Nov 1974, Washington, D. C.

Log of 6-in.-Diameter Horizontal Concrete Core No. 1
from South Abutment, Marsh Arch Bridge

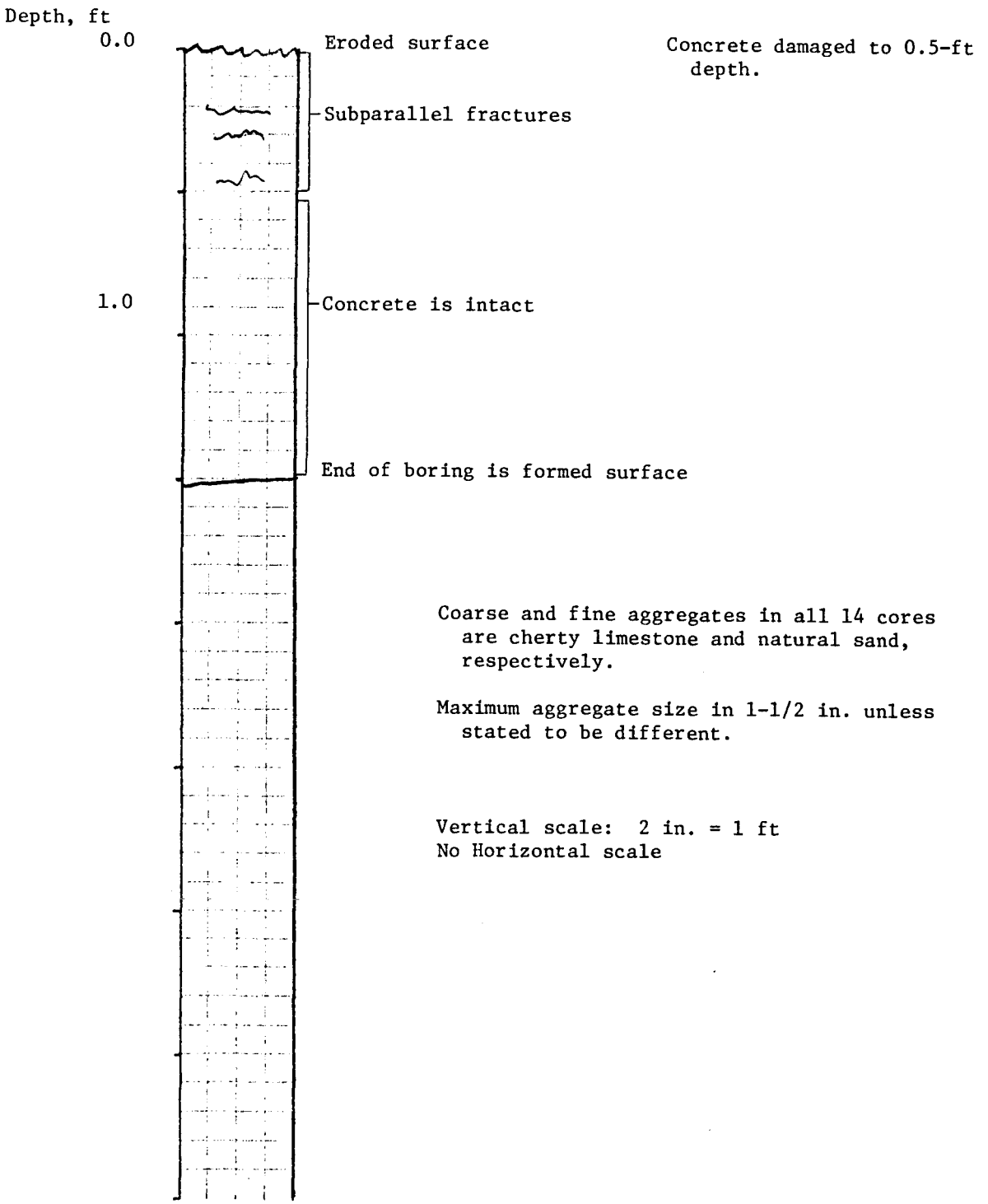

Figure A1.

Log of 6-in.-Diameter Horizontal Core No. 2
from South Abutment, Marsh Arch Bridge

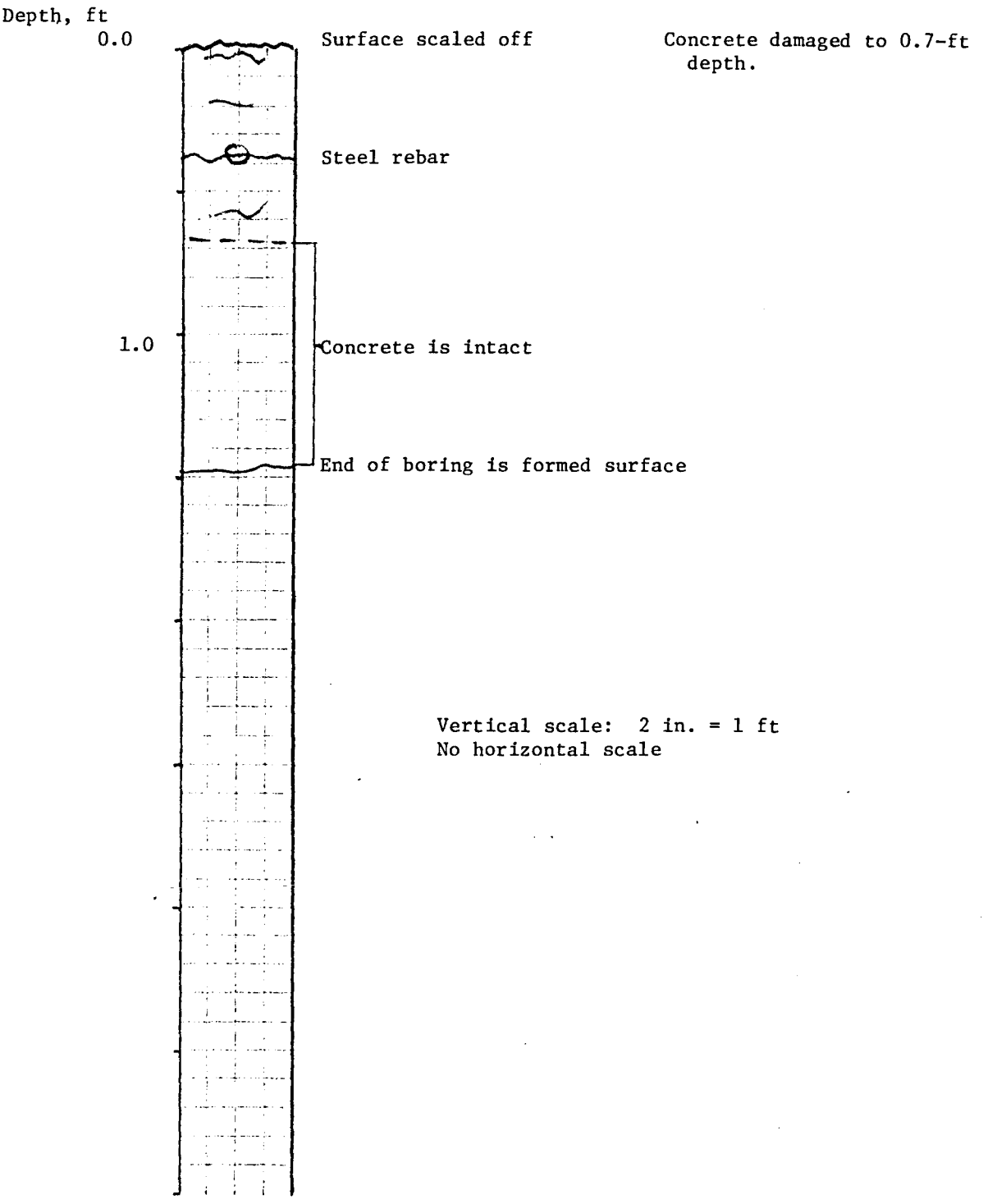

Figure A2.

Log of 6-in.-Diameter Horizontal Concrete Core No. 3
from Arch, Marsh Arch Bridge

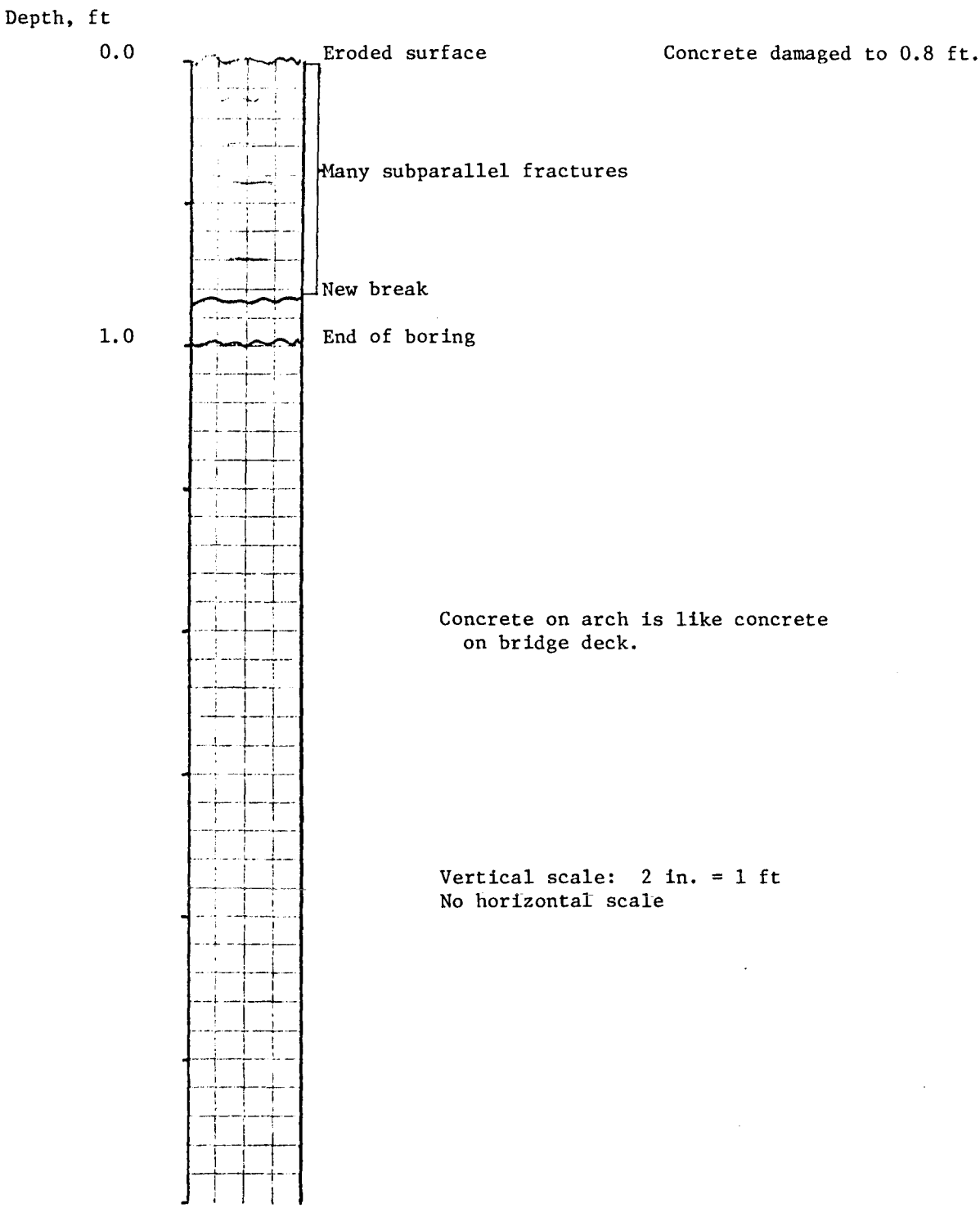

Figure A3.

Log of 6-in.-Diameter Horizontal Concrete Core No. 5
from North Abutment, Marsh Arch Bridge

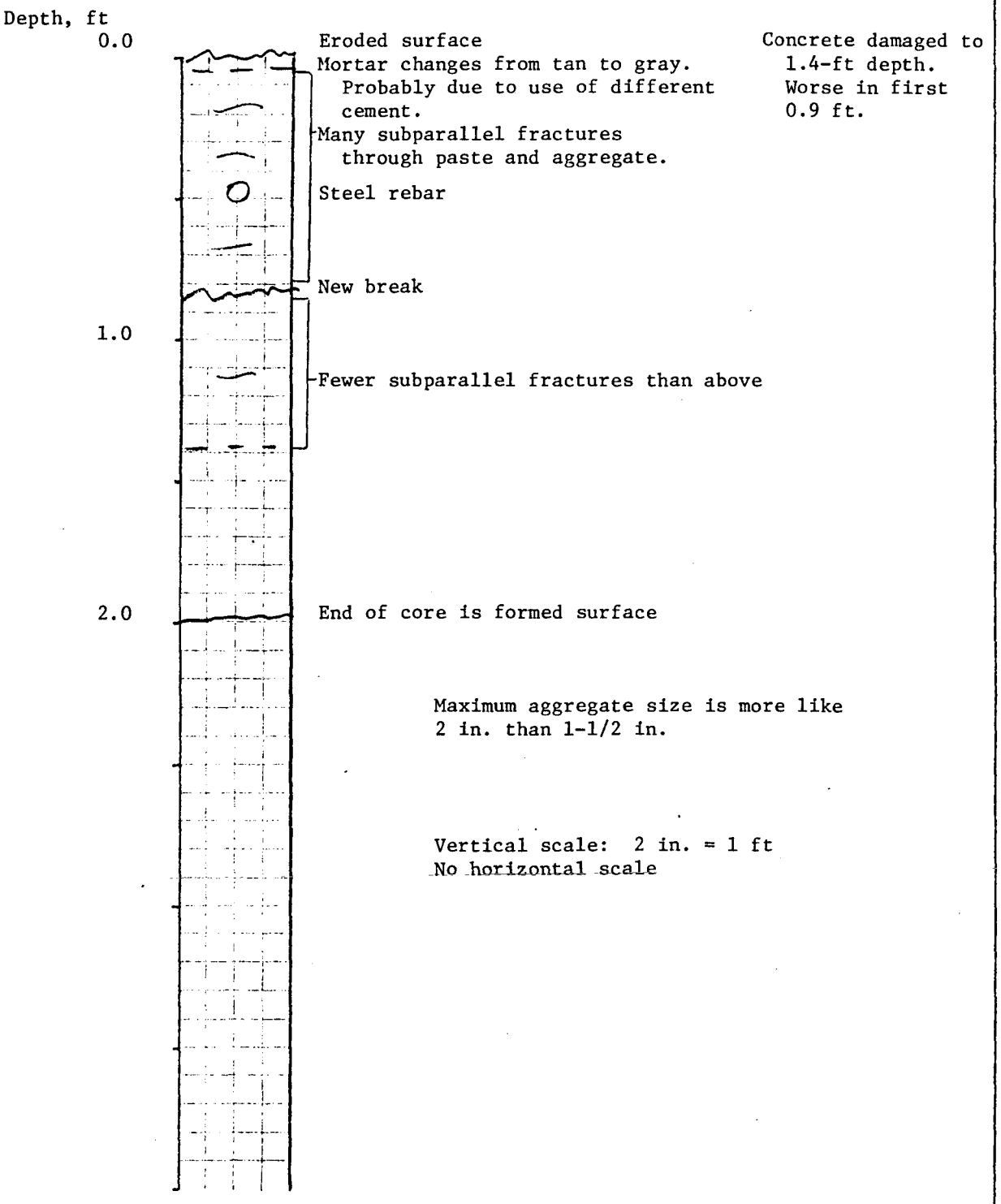

Figure A4.

Log of 6-in.-Diameter Horizontal Concrete Core No. 6
from North Abutment, Marsh Arch Bridge

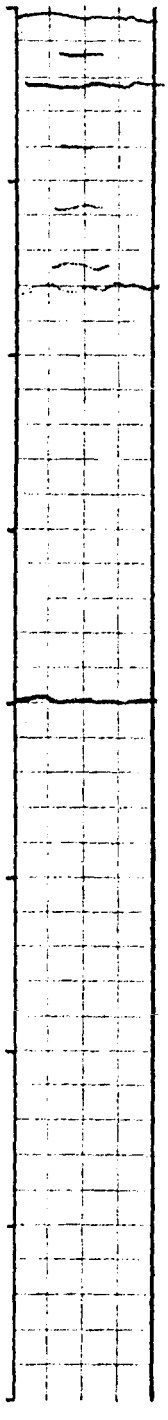

Eroded surface

Old break

Old break

Bottom of core

Closed subparallel cracks
to 0.8-ft depth

Concrete damaged to 0.8-ft depth.
Intact concrete beyond that point.

Vertical scale: 2 in. = 1 ft
No horizontal scale

Figure A5.

Log of 6-in.-Diameter Horizontal Concrete Core No. 7
from North Abutment, Marsh Arch Bridge

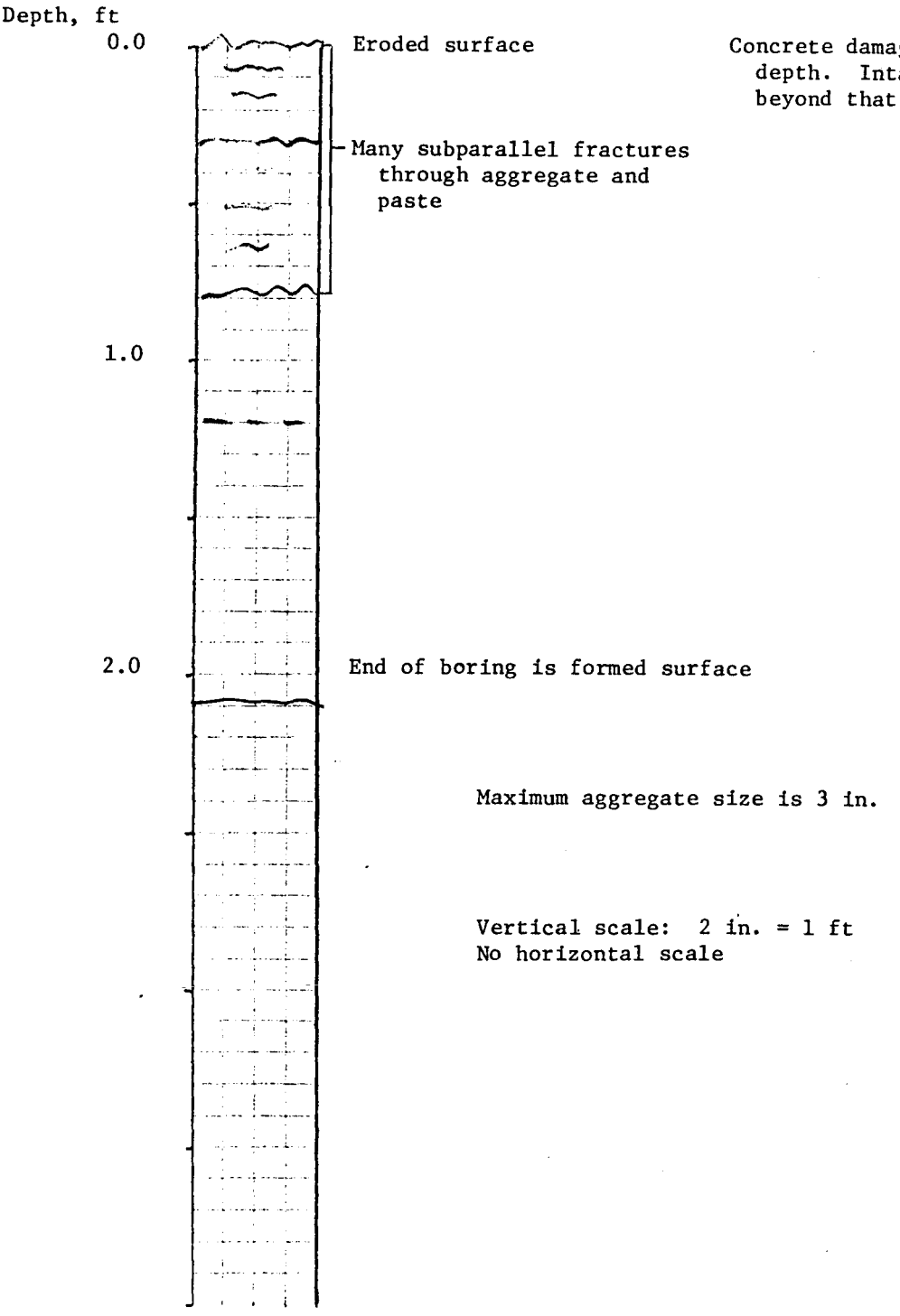

Figure A6.

Log of 6-in.-Diameter Vertical Concrete Core No. 8
Through Bridge Deck, Marsh Arch Bridge

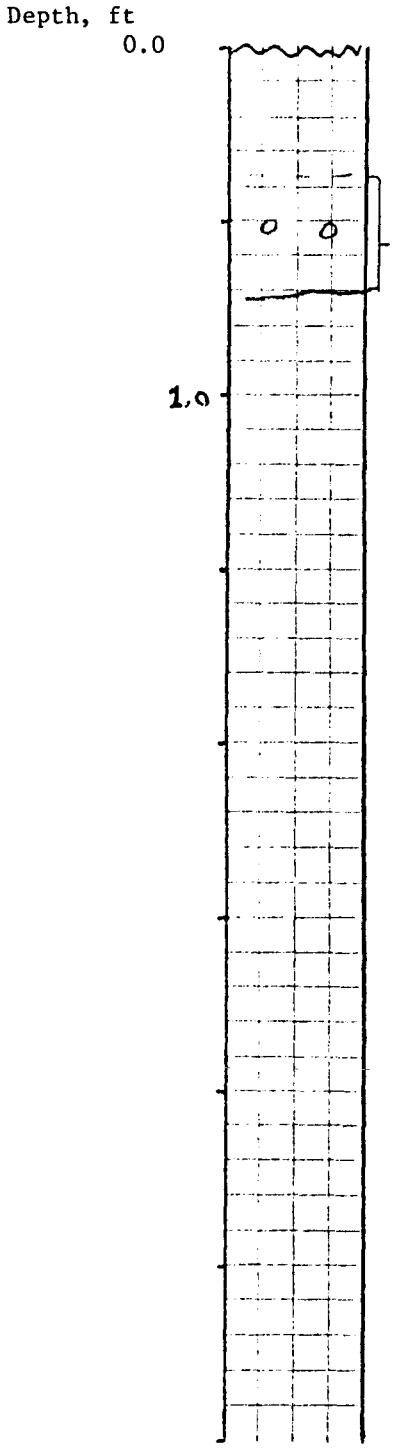

Scaled formed surface. Aside from this loss the upper 0.4 ft of core is intact. Approximately the lower half of the core is damaged.

Steel rebars
Minor subparallel fractures through aggregate and paste
Bottom of deck

Frost damage appears to be from bottom up.

Approximately the lower 6 mm of the core is gray shotcrete with a thin (about 1 mm) white mortar coating.

Vertical scale: 2 in. = 1 ft
No horizontal scale

Figure A7.

Log of 6-in.-Diameter Vertical Concrete Core No. 9
Through Bridge Deck, Marsh Arch Bridge

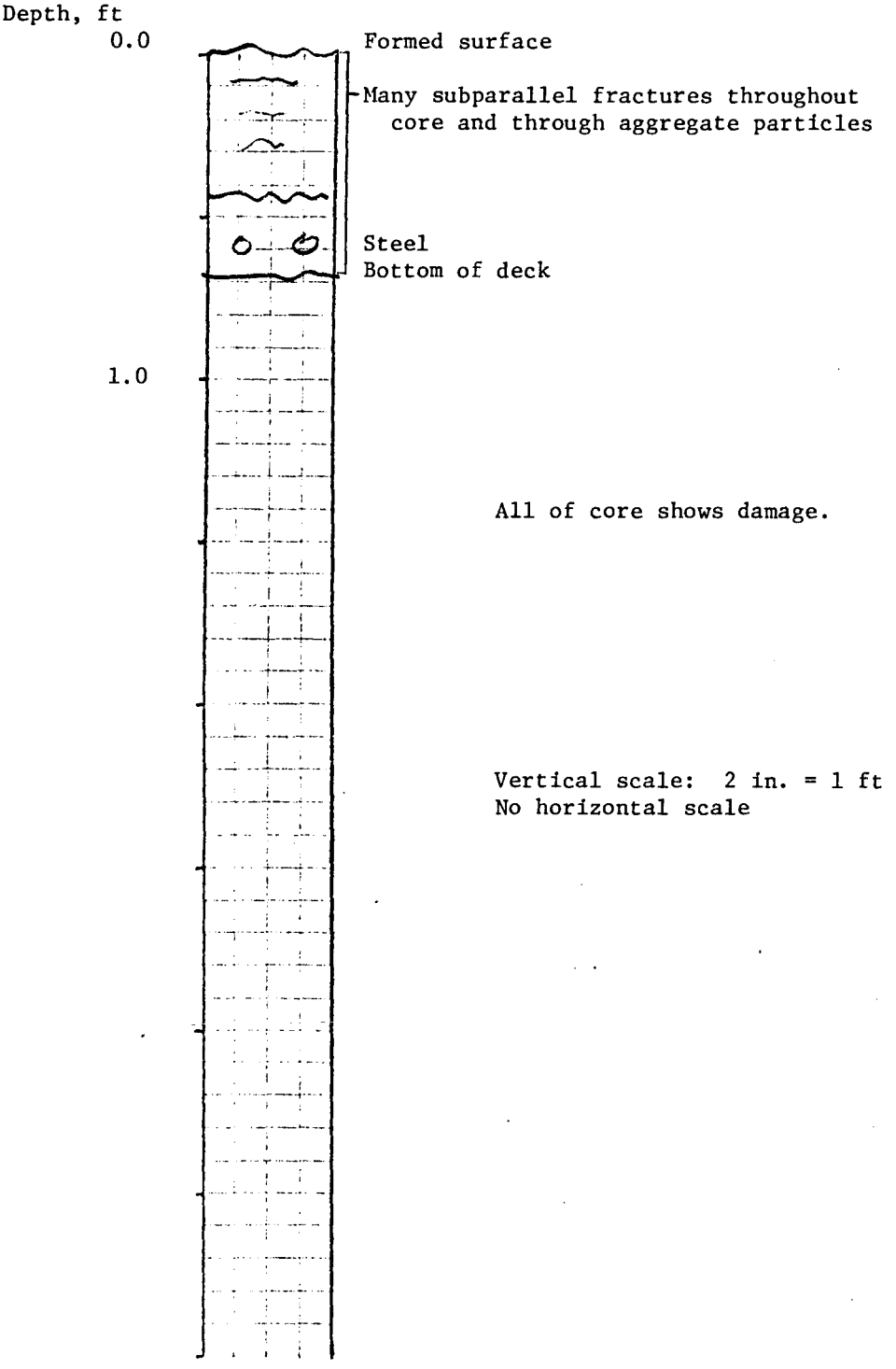

Figure A8.

Log of 6-in.-Diameter Vertical Concrete Core No. 10
Through Bridge Deck, Marsh Arch Bridge

Depth, ft

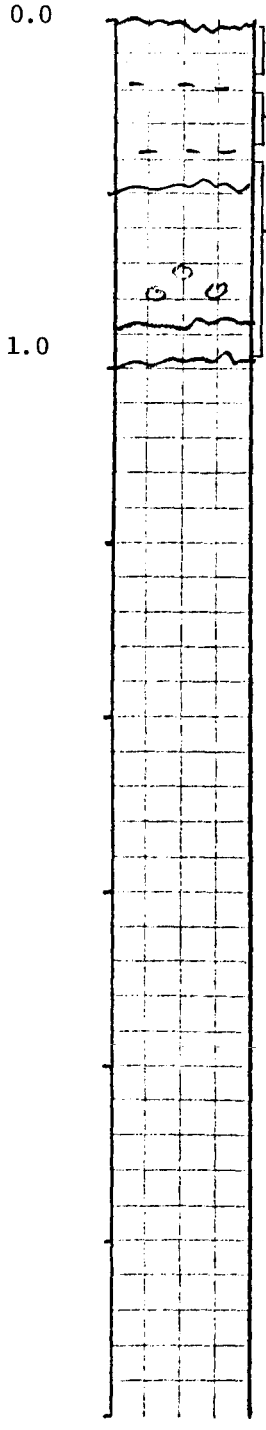

Eroded surface
Asphalt; tight contact with concrete
Mortar cap, some subparallel cracks
Heavy subparallel fracturing of concrete
Rusting of rebars may have caused break
Bottom of deck

Core is topped with asphalt and bottomed with about 9 mm of shotcrete with a thin (1 mm) white mortar coating. Essentially all of the concrete is damaged.

Vertical scale: 2 in. = 1 ft
No horizontal scale

Figure A9.

Log of 6-in.-Diameter Vertical Concrete Core No. 11
Through Bridge Deck, Marsh Arch Bridge

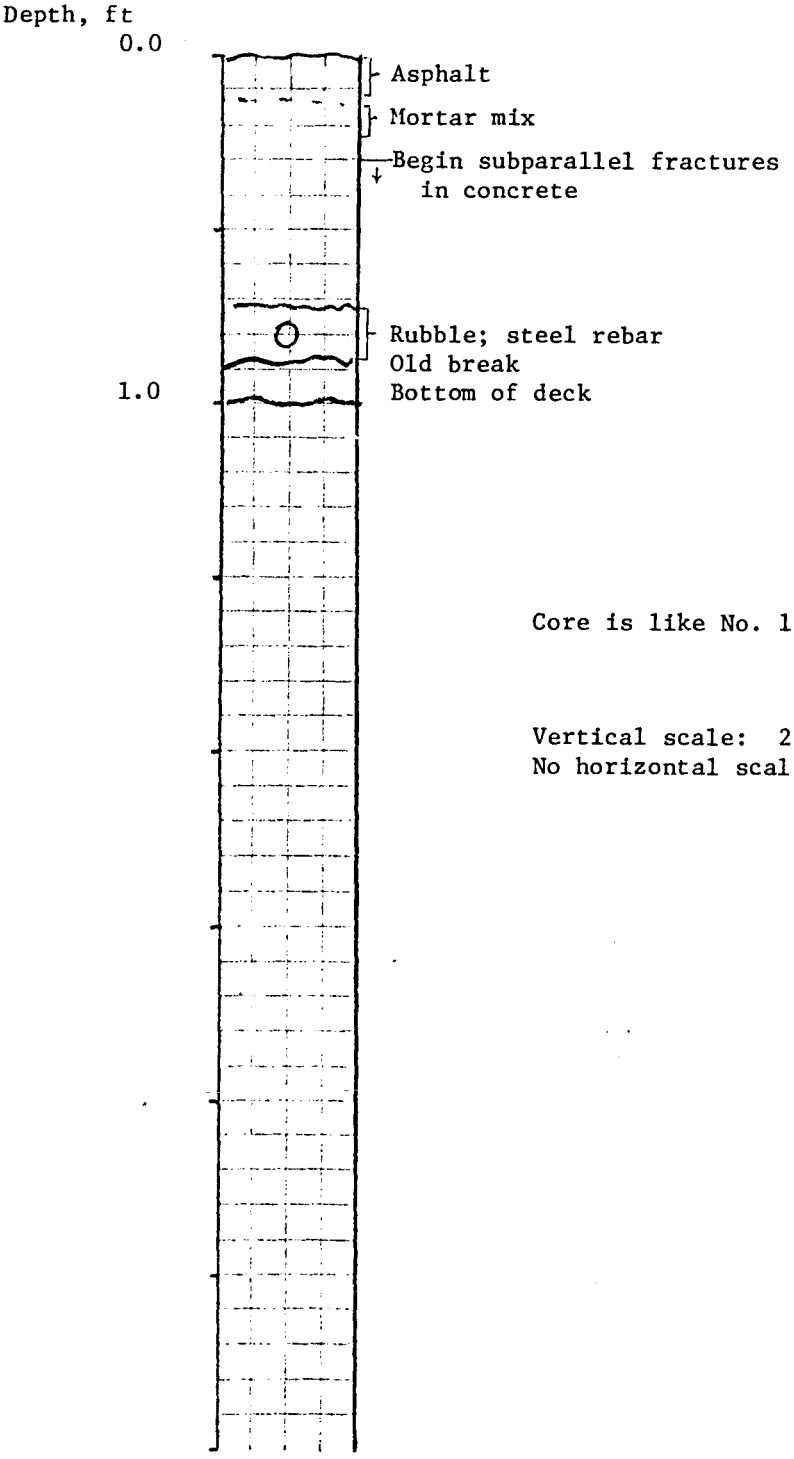

Core is like No. 10.

Vertical scale: 2 in. = 1 ft
No horizontal scale

Figure A10.

Log of 6-in.-Diameter Vertical Concrete Core No. 12
Through Bridge Deck, Marsh Arch Bridge

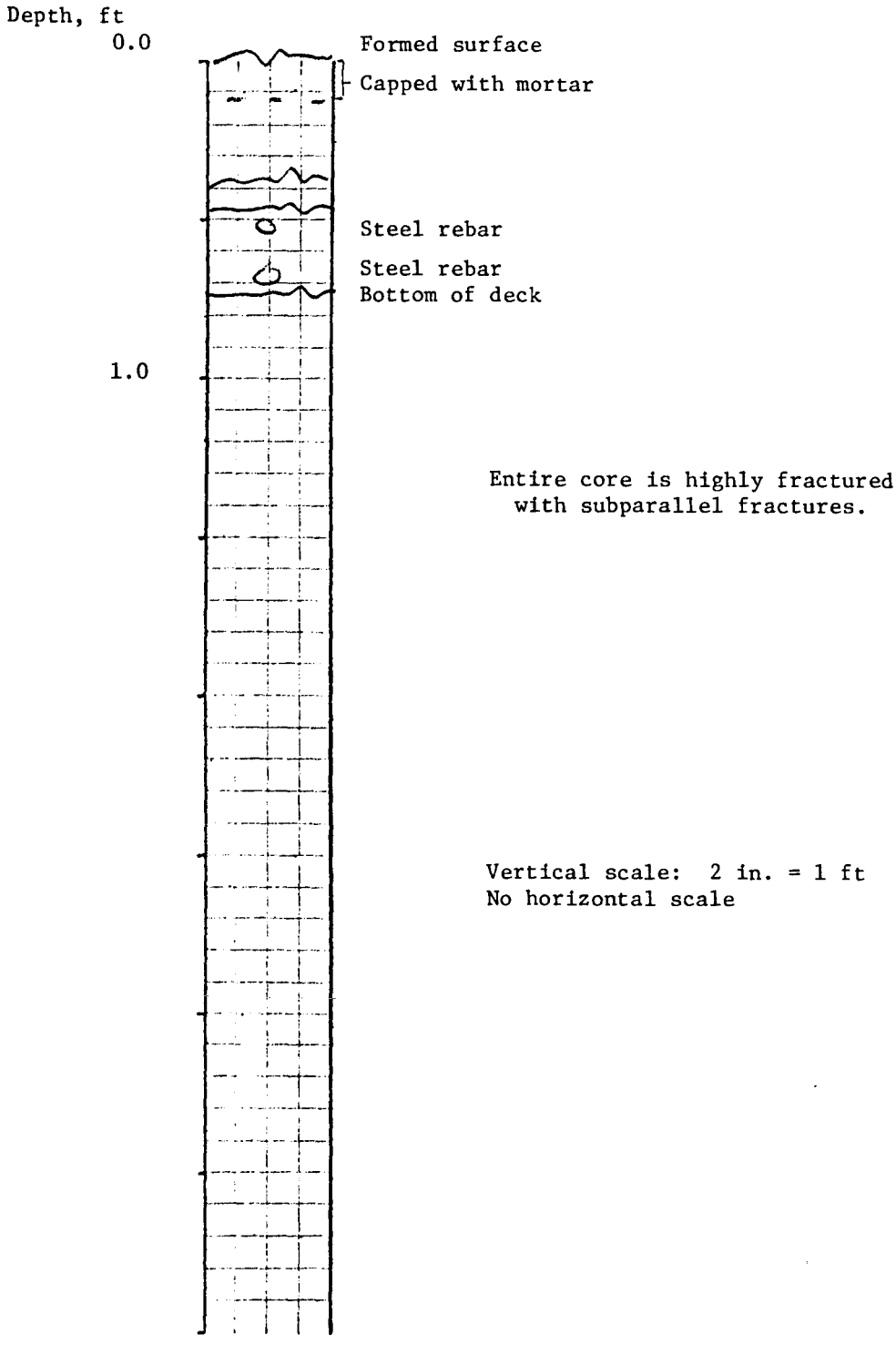

Figure A11.

Log of 6-in.-Diameter Vertical Concrete Core No. 13
Through Bridge Deck, Marsh Arch Bridge

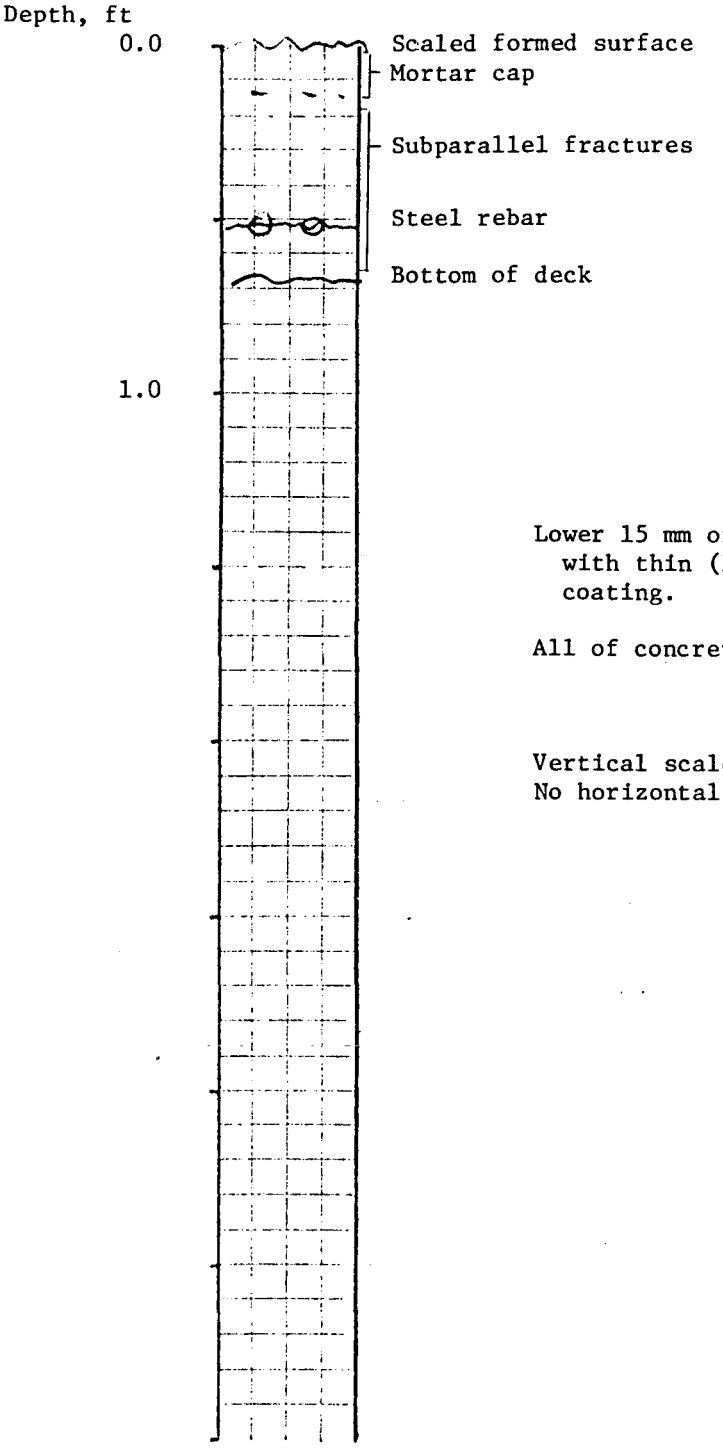

Lower 15 mm of deck is gray shotcrete with thin (1 mm) white mortar coating.

All of concrete is damaged.

Vertical scale: 2 in. = 1 ft
No horizontal scale

Figure A12.

Log of 6-in.-Diameter Vertical Concrete Core No. 14
Through Bridge Deck, Marsh Arch Bridge

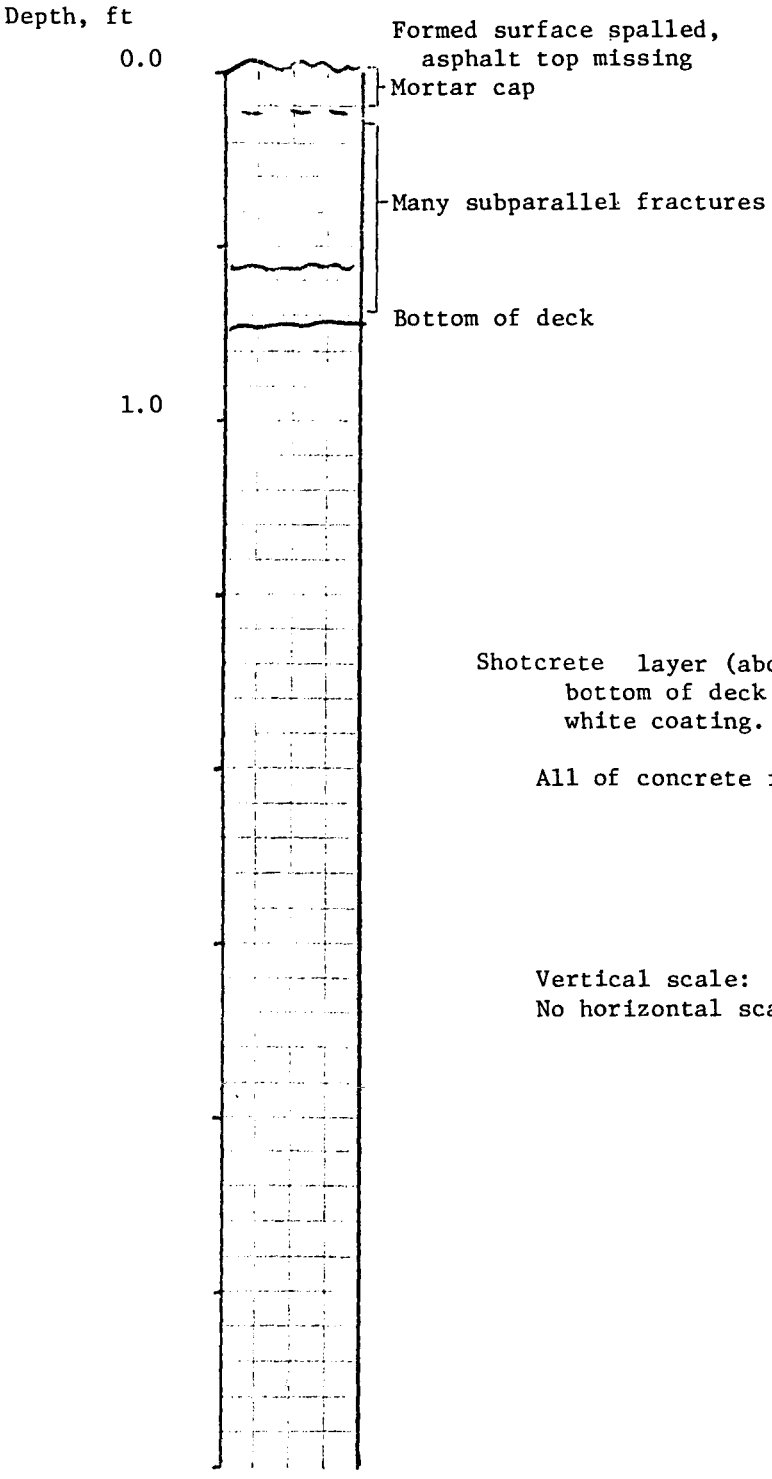

Shotcrete layer (about 6 mm thick) on bottom of deck with the usual white coating.

All of concrete is damaged.

Vertical scale: 2 in. = 1 ft
No horizontal scale

Figure A13.

Log of 6-in.-Diameter Vertical Concrete Core No. 15
Through Bridge Deck, Marsh Arch Bridge

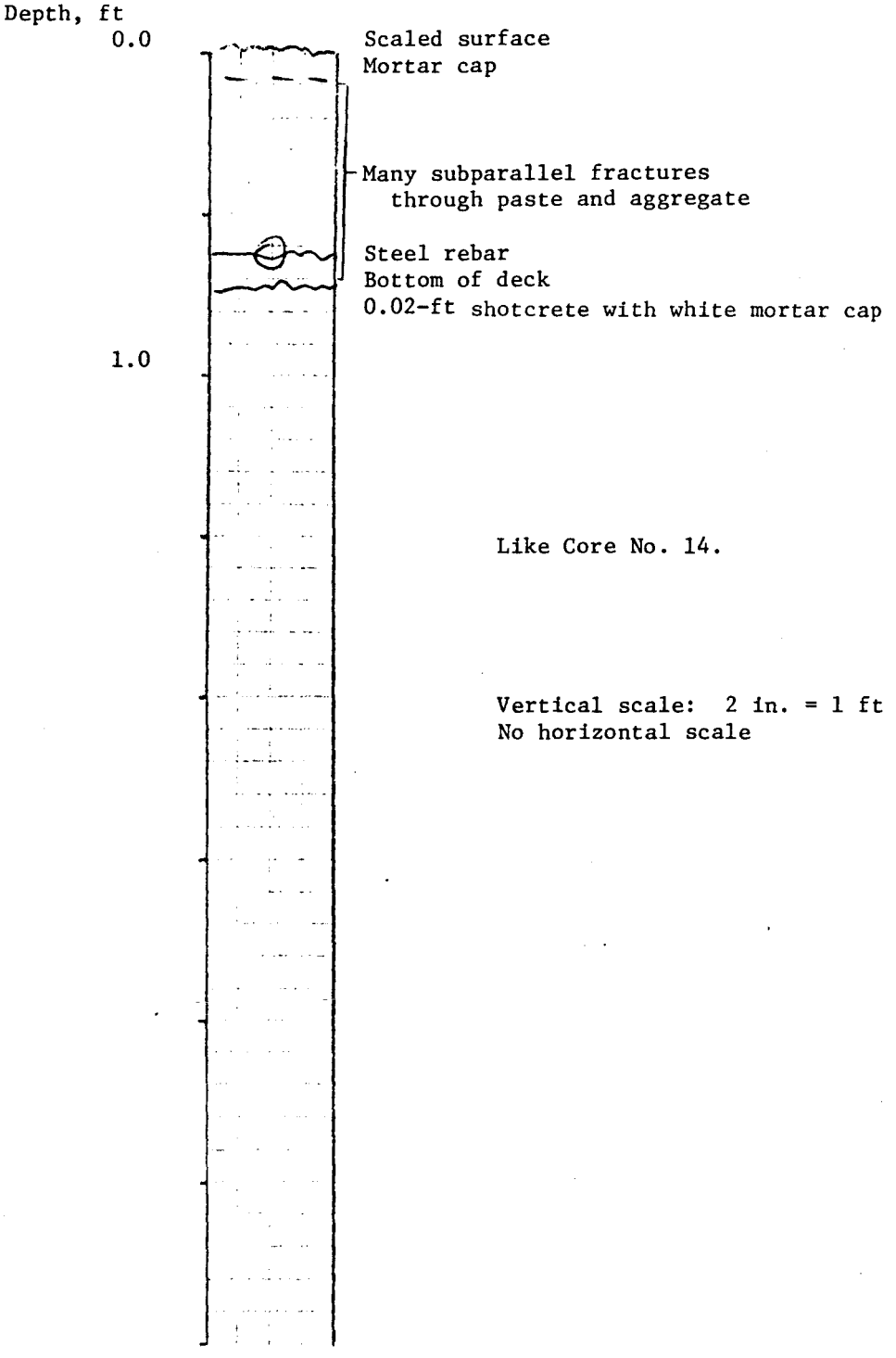

Figure A14.

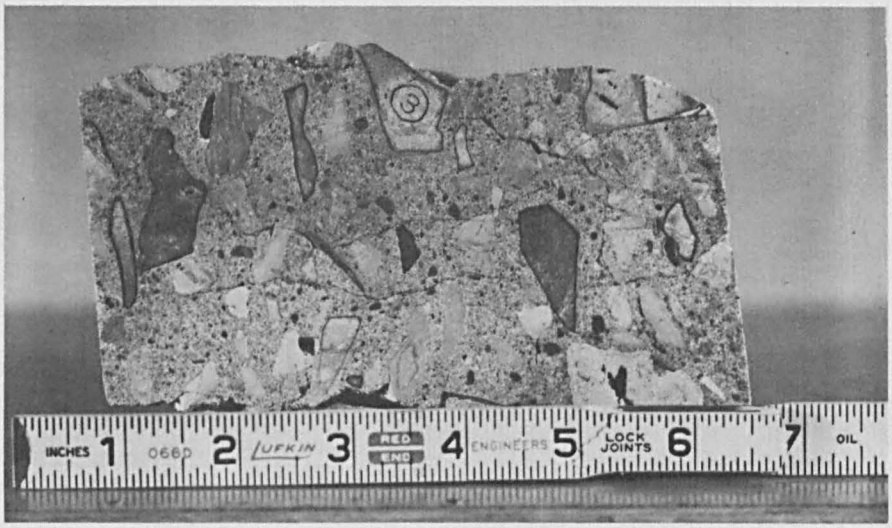

a. Sawed and ground surface of a portion of core 3 from an arch section. The aggregate particles showing dark rims are chert that have reacted in the alkali-silica reaction. About half normal size.

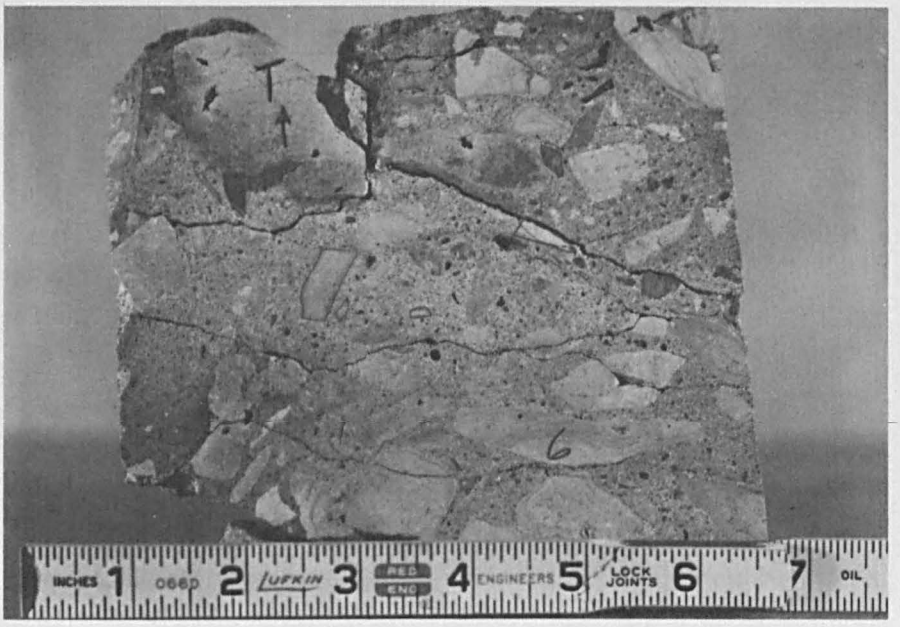

b. Section of core 6 from the North Abutment prepared as above. The surface shows several limestone coarse aggregate particles with reaction rims (upper, lower areas). These were involved in an alkali-carbonate rock reaction.

Figure A15. The sawed and ground surfaces of portions of cores 3 and 6.

APPENDIX B

METHOD OF TEST FOR TOTAL CHLORIDE IN CEMENT, MORTAR, AND CONCRETE

APPENDIX B

METHOD OF TEST FOR TOTAL CHLORIDE IN CEMENT, MORTAR, AND CONCRETE

1. Scope

1.1 This method covers a procedure for the determination of the total chloride content of dry or hydrated portland cement, mortar, or concrete. The method is limited to materials that do not contain sulfides, but the extraction procedure, paragraphs 4.1 and 4.2 may be used for all such materials.

2. Apparatus

2.1 Chloride-ion selective electrode and manufacturer-recommended accessory solutions. The combination solid-state electrode is the most convenient and dependable of the three types available, requiring less maintenance than the single electrode or the membrane type.

2.2 A millivoltmeter or pH-meter compatible with the ion electrode.

2.3 Magnetic stirrer and teflon stirring bars.

2.4 Burette with 0.1 ml graduations.

3. Reagents

3.1 Concentrated HNO_3 (sp. gr. 1.42).

3.2 Sodium chloride, NaCl, reagent grade (primary standard).

3.3 Standard 0.01 N NaCl solution. Dry reagent grade NaCl in an oven at 105 C. Cool, weigh out 0.5844 grams, dissolve in distilled H_2O, and transfer to a 1-litre volumetric flask. Make up to the mark with distilled H_2O and mix.

3.4 Standard 0.01 N $AgNO_3$ solution. Weigh 1.7 grams of reagent grade $NgNO_3$, dissolve in distilled H_2O, filter into a 1-litre brown glass bottle, fill, and mix thoroughly. Standardize with 20 ml of the NaCl solution by the titration method given in paragraphs 4.4 and 4.5.

3.5 Standard 0.025 N $AgNO_3$ solution. Prepare as for the 0.01 N solution, but use 4.25 grams of $AgNO_3$. Standardize with 50 ml of the NaCl solution.

4. Procedure

4.1 Weigh to the nearest milligram a 1- to 3-gram powdered sample representative of the material under test. Add 10 ml of distilled H_2O, swirling to bring the powder into suspension. Add 3 ml of concentrated HNO_3 with continued swirling until the cement is completely decomposed. Break up any lumps with a stirring rod and dilute with hot H_2O to 50 ml if necessary. If the solution is not acid at this point, add only enough HNO_3 to produce a red color with methyl orange indicator. The 3 ml of concentrated HNO_3 originally added is usually sufficient to complete the

solution of as much as 3 grams of cement paste, but may not be enough for some concrete samples containing carbonate aggregates.

4.2 Heat the acid solution or slurry to boiling on a hot plate at medium heat and boil for about 1 minute. Remove from the hot plate and filter into a 250-ml beaker. To facilitate the filtration of the gelatinous residue, use a double thickness of filter paper, consisting of a medium-porosity paper under one of high porosity. Decant the clear solution, wash the residue in the beaker once, then transfer it into the filter paper with the aid of hot distilled H_2O. Wash the filter paper thoroughly (5 to 10 times) with the hot H_2O. Allow the filtrate to cool to room temperature.

4.3 Fill the chloride electrode with the solution(s) recommended by the manufacturer, plug it into the millivoltmeter, and determine the approximate position of the equivalence point by immersing the electrode in a beaker of distilled H_2O. Note the approximate millivoltmeter reading (which can be unsteady in H_2O).

4.4 Remove the beaker of distilled H_2O, wipe the electrode with absorbent paper, and immerse the electrode in the sample solution. The entire assembly should be placed on a magnetic stirring device. Add and record the volume of successive increments of standard $AgNO_3$ solution from the burette (0.01 N or 0.025 N, depending on the quantity of chloride expected), recording the millivoltmeter reading after each addition. The increment of $AgNO_3$ solution should be enough to change the reading by 5 to 10 mv. As the titration proceeds, smaller increments of $AgNO_3$ solution will be sufficient to deflect the needle by this amount, until increments of only 0.1 or even 0.05 ml are effective (starting about 40 mv from the equivalence point). After the equivalence point has been reached, the needle deflections will begin to decrease with equal increments of $AgNO_3$ solution. Continue the titration past the equivalence point long enough to establish that the meter deflections are decreasing progressively, usually 40 to 60 mv past the equivalence point. The endpoint of the titration is the point of inflection of a curve of millivoltmeter readings vs. volume of $AgNO_3$ solution added. This point may usually be estimated accurately without plotting the curve. It is the midpoint of the increment which produced the largest deflection per unit of silver nitrate added and usually occurs near the approximate equivalence point of the electrode.

(Note) If the millivoltmeter deflections are not symmetrical on opposite sides of the estimated largest deflection, the endpoint may be displaced 0.01 to 0.03 ml from the midpoint of the largest deflection in the direction of skew. The degree of asymmetry thus may be used to establish the endpoint within 0.01 ml when the increments of $AgNO_3$ solution are 0.1 ml.

(Note) In acid solutions the equivalence point, as well as the other millivoltmeter readings, is less positive than it is in distilled H_2O. In alkaline solutions, it is more positive.

5. Calculations

5.1 The percent chloride in the sample = $\frac{35.453\ VN}{10\ W}$

where V is the volume of silver nitrate solution, in ml, added up to the endpoint,

N is the normality of the silver nitrate solution

W is the weight of the sample in grams.

In accordance with ER 70-2-3, paragraph 6c(1)(b), dated 15 February 1973, a facsimile catalog card in Library of Congress format is reproduced below.

Liu, T C
Engineering condition survey and structural investigation of Marsh Arch Bridge, Fort Riley, Kansas, by T. C. Liu. Vicksburg, U. S. Army Engineer Waterways Experiment Station, 1977.
1 v. (various pagings) illus. 27 cm. (U. S. Waterways Experiment Station. Miscellaneous paper C-77-1)
Prepared for U. S. Army Engineer District, Kansas City, Kansas City, Mo.
Includes bibliography.

1. Arch bridges. 2. Bridges (Structures). 3. Concrete bridges. 4. Concrete cracking. 5. Concrete deterioration. 6. Concrete failure. 7. Marsh Arch Bridge. 8. Structural analysis. I. U. S. Army Engineer District, Kansas City. (Series: U. S. Waterways Experiment Station, Vicksburg, Miss. Miscellaneous paper C-77-1)
TA7.W34m no.C-77-1